



## Large-scale physical modelling of wave damping of brushwood mattresses





**Large-scale physical modelling of  
wave damping of brushwood  
mattresses**

ir. P. Steeg  
dr. B.K. Wesenbeeck





**Title**

Large-scale physical modelling of wave damping of brushwood mattresses

**Client**

Deltares MT

**Pages**

21 (excl. appendices)

**Keywords**

Floating breakwater, floating wetlands, building with nature, large-scale physical model, flume experiment, brushwood, wave damping, transmission coefficient

**Summary**

Floating wetlands are commonly used to enhance ecological value and water quality in water systems that are severely impacted by humans. These wetlands could also be applied to reduce hydraulic forcing and thereby aid in coastal protection. Integrating these functions of biological elements in hydraulic engineering designs is a new and promising field, known as Building with Nature or Eco-engineering. However, many knowledge gaps still need to be filled to make this possible. One of these gaps concerns quantification of hydraulic properties of biological elements. To determine the wave damping characteristics of floating brushwood mattresses, large-scale physical modelling in the Deltares Delta Flume was performed.

Tests with following characteristics were performed:




*Hydraulic conditions*

Water depth	$d = 4$ m
Significant wave height	$H_s = 0.20$ m, 0.40 m; 0.60 m
Wave steepness	$s_{o,p} = 0.02$ ; 0.03; 0.04
Number of waves per test-run	$N \approx 1000$
Type of waves	irregular (JONSWAP spectrum)

*Mattresses*

Length	$w = 4$ m; 12 m
Thickness	$D \approx 0.45$ m
Thickness (under water)	$d \approx 0.30$ m

The transmission coefficient was determined for each test-run. Based on this empirical data a set of formulas have been derived which predicts the transmission coefficient as function of mattress characteristics (mattress length, under water depth) and hydraulic conditions (wave length, water depth). In general, brushwood mattresses function well for wave dampening, but design of mattresses needs to be improved for application in the field.

Version	Date	Author	Initials	Review	Initials	Approval	Initials
Draft	Nov. 2010	Ir. P. van Steeg Dr. B. van Wesenbeeck		Dr. B. Hofland		Dr. M.R.A. van Gent	
Final	July 2011	Ir. P. van Steeg Dr. B. van Wesenbeeck		Dr. B. Hofland		Dr. M.R.A. van Gent	

**State**

final



## Contents

<b>List of Tables</b>	<b>v</b>
<b>List of Figures</b>	<b>vii</b>
<b>List of Photographs</b>	<b>ix</b>
<b>List of Symbols</b>	<b>xi</b>
<b>1 Introduction</b>	<b>1</b>
1.1 General	1
1.2 Background	1
1.3 Outline	2
<b>2 Theoretical background</b>	<b>3</b>
<b>3 Physical model tests</b>	<b>5</b>
3.1 Test set-up	5
3.1.1 Test facility	5
3.1.2 Coordinate system	5
3.1.3 General test set-up	5
3.2 Materials	6
3.2.1 Dimensions of mattresses	6
3.2.2 Fixation of mattresses	6
3.3 Instrumentation: wave measurements	6
3.4 Hydraulic conditions and test programme	8
3.5 Description and visual observation	8
3.5.1 Test Series 200 ( $w = 12$ m)	8
3.5.2 Test Series 300 ( $w = 4$ m)	9
3.5.3 Test Series 600 (no mattresses)	9
3.6 Results: wave measurements	9
<b>4 Analysis</b>	<b>11</b>
4.1 Wave height exceedance curves and energy density spectra	11
4.2 Transmission coefficient	12
4.3 Prediction of transmission, reflection and dissipation coefficient	15
4.4 Summary prediction model	16
4.5 Restrictions of wave damping prediction model	17
4.6 Example of using prediction model	17
4.7 Strength aspects	18
<b>5 Conclusions and recommendations</b>	<b>19</b>
5.1 Conclusions	19
5.2 Recommendations	19
5.2.1 Wave damping characteristics	19
5.2.2 Other engineering aspects: strength and anchorage	20
<b>6 References</b>	<b>21</b>



**Appendices**

**A Tables**

**B Figures**

**C Photographs**

**D Exceedance curves and energy density spectra**

**E Theoretical background: determination of reflected, transmitted and dissipated wave energy**

**F Theoretical derivation of  $\chi$**

**G Theoretical determination of dissipation coefficient  $C_{diss}$**

**H Calculation tool**



## List of Tables

### *In text*

Table 3.1 Overview test series	5
Table 3.2 Overview of wave conditions (target values) for test series T200 (w = 12 m)	8
Table 3.3 Overview of wave conditions (target values) for test series T300 (w = 4 m)	8
Table 3.4 Overview of wave conditions (target values) for test series T600 (no mattresses)	8
Table 4.1 Overview of comparison of wave height exceedance curves and energy spectra	12
Table 4.2 Range of tested conditions	17
Table 4.3 Range of tested conditions (dimensionless)	17
Table 4.4 Hydraulic conditions of test case	17
Table 4.5 Mattress conditions of tests case	18
Table 4.6 Results of test case	18
Table 4.7 Warnings given for test case	18

### *In appendices*

Table A.1 Measured wave conditions	
Table A.2 Reflection, transmission and dissipation coefficients	
Table A.3 Coordinates of all objects	
Table A.4 Characteristics of mattresses	
Table E.1 Overview determination incident, transmitted and reflected wave energy for an irregular wave field	





## List of Figures

### *In text*

Figure 2.1 Classification of floating structures (after PIANC, 1994)	3
Figure 3.1 Overview test set-up	5
Figure 3.2 Schematisation of determination of the wave energy components	7
Figure 4.1 Wave spectra Test T204 ( $s_{o,p} = 0.02$ , $H_s = 0.4$ m)	11
Figure 4.2 Wave spectra Test T205 ( $s_{o,p} = 0.03$ , $H_s = 0.4$ m)	11
Figure 4.3 Wave spectra Test T202 ( $s_{o,p} = 0.04$ , $H_s = 0.4$ m)	11
Figure 4.4 Wave spectra Test T202 ( $H_s = 0.4$ m, $w = 12$ m)	12
Figure 4.5 Wave spectra Test T302 ( $H_s = 0.4$ m, $w = 4$ m)	12
Figure 4.6 Transmission coefficient $C_t$ as function of $H_{m0}$ and as function of relative mattress length $w/L_p$	13
Figure 4.7 Vertical energy distribution for shallow and deep water	13
Figure 4.8 Schematisation of object blocking a wave	13
Figure 4.9 Effect of wave and structure depth (derivation in Appendix F)	14
Figure 4.10 Transmission coefficient as function of blocked wave energy $\chi_{BL}$	14
Figure 4.11 Transmission coefficient $C_t$ as function of dimensionless parameter $(w/L_p)\chi_{BL}$	15
Figure 4.12 Measured dissipation and reflection coefficients and derived trend line	15
Figure 5.1 Transmission coefficient $C_t$ as function of mattress length $w$ , wave length $L_p$ and ratio of blocked wave energy $\chi_{BL}$	19

## *In appendices*

Figure B.1 Overview of test set-up

Figure B.2 Detail of mattresses

Figure B.3 Transmission, reflection and dissipation coefficient as function of significant wave height  $H_{m0}$

Figure B.4 Transmission, reflection and dissipation coefficient as function of relative mattress length  $w/L_p$

Figure B.5 Transmission, reflection and dissipation coefficient as function of  $(w/L_p)\chi_{BL}$

Figure D.1 Exceedance curve and energy density spectra for Test T201

Figure D.2 Exceedance curve and energy density spectra for Test T202

Figure D.3 Exceedance curve and energy density spectra for Test T204

Figure D.4 Exceedance curve and energy density spectra for Test T205

Figure D.5 Exceedance curve and energy density spectra for Test T203

Figure D.6 Exceedance curve and energy density spectra for Test T301

Figure D.7 Exceedance curve and energy density spectra for Test T302

Figure D.8 Exceedance curve and energy density spectra for Test T305

Figure D.9 Exceedance curve and energy density spectra for Test T308

Figure D.10 Exceedance curve and energy density spectra for Test T601

Figure D.11 Exceedance curve and energy density spectra for Test T603

Figure E.1 Schematisation of the model set-up for an irregular wave field

Figure F.1 Schematisation of fixed structure blocking wave energy

Figure G.1 Dissipation of energy on a porous segment

Figure G.2 Graphical presentation of dissipation coefficient based on Eq. (6.9)

Figure H.1 Impression of calculation tool (page 1/2)

Figure H.2 Impression of calculation tool (page 2/2)

## List of Photographs

### *In appendices*

- Photo C.1 Construction of mattresses (1)
- Photo C.2 Construction of mattresses (2)
- Photo C.3 Mattresses after construction
- Photo C.4 Mattresses during wave experiments
- Photo C.5 Mattresses during wave experiment (2)
- Photo C.6 Mattresses with a total length of 4 m
- Photo C.7 Damage on mattresses after a test (1)
- Photo C.8 Damage on mattresses after a test (2)



## List of Symbols

Symbol	Unit	Description
$B_{str}$	m	width of structure
$B_{fl}$	m	width of flume
$C_{diss}$	-	dissipation coefficient
$C_r$	-	reflection coefficient
$C_t$	-	transmission coefficient
$d$	m	depth of structure under water
$D$	m	height of structure
$E_{diss}$	N/m	dissipated wave energy
$E_i$	N/m	incident wave energy
$E_r$	N/m	reflected wave energy
$E_t$	N/m	transmitted wave energy
$f$	-	coefficient
$f$	Hz	frequency
$g$	m/s <sup>2</sup>	acceleration due to gravitational forces
$h$		water depth
$H_s$	m	significant wave height based on spectral wave period
$k$	(rad/m)	wave number
$L_{flume}$	m	length of the flume
$L_p$	m	local wave length based on $T_p$
$L_{o,p}$	m	wave length at deep water based on $T_p$
$m$	kg	mass
$n$	-	number of individual mattresses
$N$	-	number of waves in a wave field
$p$	-	percentage of energy
$t$	s	time
$T_p$	s	peak wave period
$w$	m	length of floating structure in the direction of the waves
$X$	m	horizontal distance from the wave board in neutral position
$Y$	m	horizontal distance from the western flume wall
$Z$	m	vertical distance from SWL (upward is positive)
$\alpha$	-	ratio between the transmitted and reflected wave energy $\alpha = E_{diss}/E_r$
$\gamma$	-	peak enhancement factor of wave spectrum
$X_{BL}$	-	ratio of blocked energy
$X_t$		ratio of transmitted energy

## Commonly used indexes

<b>Symbol</b>	<b>Description</b>
A	index to relate the concerned parameter to waves travelling from the wave board to the wall
ARC	Active reflection compensation of the wave board
B	index to relate the concerned parameter to reflected waves travelling from the wall to the wave board
BL	blocked wave energy
bs	breaking on smooth concrete 1:4 slope
C	index to relate the parameter to re-reflected waves travelling from the floating structure to the wall
diss	dissipated
fl	flume
i	incident
r	reflected
rr	re-reflected
t	transmitted
GHM	wave height meter at seaward side of the mattresses
WHM	wave height meter at landward side of the mattresses
1	position: seaside of mattresses (or GHM 11,12, 13)
2	position: landward side of mattresses (or WHM 1, 2, 3)



# 1 Introduction

## 1.1 General

Traditional gradients between land and water are disappearing in delta areas world wide. To realize safety from flooding building of hard structures such as levees, dams and dikes has become common practice along rivers, lakes and in coastal areas. In the Netherlands especially large fresh water lakes have lost their shallow water habitats and gradual transitions between land and water. Consequently, species that inhabit these zones are decreasing. Additionally, natural fluctuations in water level are often absent, making ecosystem dynamics of temporarily submerged wetlands impossible. This results in deterioration of these habitats. Wetland vegetation, submerged vegetation and filter feeders are not only of ecological importance but also play a decisive role in water purification and entrapment of suspended solids. This explains why construction of floating wetlands is becoming a popular restoration measure that is applied in open areas amidst natural wetlands areas, but also in urban areas.

In fresh water systems fixed water levels do not only have negative influences on the water system but also cause shoreline erosion, which affects management and maintenance of shorelines. To use floating wetlands for wave attenuation is a new and promising application. This application fits in other ecosystem based coastal protection measures that are being explored by Deltares under running Building with Nature or Eco-engineering projects. Multiple ecosystem services that can be combined by adopting such an approach make these solutions attractive and cost-efficient. Although Building with Nature solutions seem promising, quantitative data supporting their effectiveness is not always available. Especially on wave damping properties of biological elements in situ measurements are sparse.

Pilot experiments with using floating brushwood mattresses for establishment of reed were executed in 2009 in Lake Marken (the Netherlands). The aim was to protect shorelines from continuous impact of small waves and to create a sediment sink. However, the original design did not withstand field conditions and lost buoyancy within two months. Therefore, the mattresses were removed from the site sooner than anticipated. However, the original idea is still considered valuable and feasible. Therefore, the current study focuses on collection of wave damping properties of floating brushwood mattresses. This is tested in a large-scale flume facility with a range of wave conditions. Experiments and analyses were set up to provide general relationships between length and thickness of mattresses and their wave damping abilities. Deriving general relationships between wave characteristics and mattress properties will allow scaling up of results. This enables application of results to other situations, although testing of newly derived values and designs is still recommended to determine whether general relationships remain valid.

## 1.2 Background

Within the Deltares research Theme "Water safety" of the Deltares Strategic Research program, several innovative concepts with respect to water retaining are studied. One of the aims of this research program is to explore wave damping aspects of ecological materials. In 2010, these explorations were started by exploring wave-damping properties of brushwood mattresses in large-scale flume facilities.

This report describes in detail the set-up and execution of large-scale physical model tests in the Deltares Delta Flume and subsequent data analyses.

The physical model tests were performed in the Delta Flume of Deltares under supervision of ir. P. van Steeg<sup>1</sup> and Dr. B.K. van Wesenbeeck<sup>2</sup> with assistance of mr. A. Scheer, mr. P.A. Wiersma, mr. L. Tulp and mr. J.H. Ouderling. Dr. B. Hofland contributed significantly with respect to derivation of design formulas. This report is written by ir. P. van Steeg and Dr. B.K. van Wesenbeeck and is reviewed by Dr. B. Hofland.

### 1.3 Outline

Chapter 2 summarizes the theoretical background on wave damping by floating breakwaters. The model set-up is given in Chapter 3, followed by results, analysis of results and development of a prediction method in Chapter 4. Chapter 5 deals with main conclusions and recommendations on design of mattresses, applications and knowledge gaps.

---

1. Deltares, [paul.vansteeg@deltares.nl](mailto:paul.vansteeg@deltares.nl)

2. Deltares, [bregje.vanwesenbeeck@deltares.nl](mailto:bregje.vanwesenbeeck@deltares.nl)

## 2 Theoretical background

An analogy between floating wetlands and floating breakwaters is made concerning wave attenuation characteristics. In PIANC (1994), floating breakwaters are schematically divided into two groups:

- Reflective structures (reflect the wave energy)
- Dissipative structures (dissipate the wave energy)

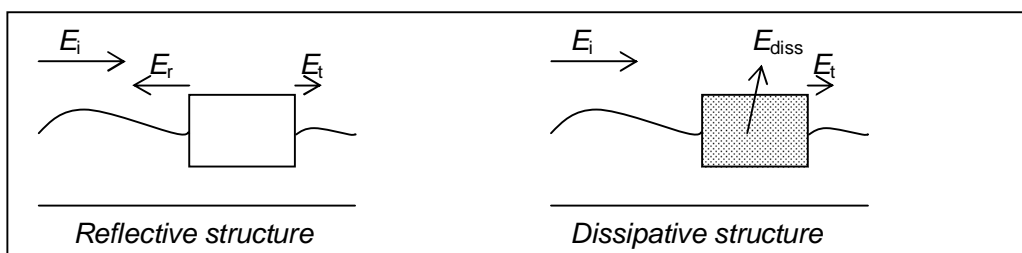


Figure 2.1 Classification of floating structures (after PIANC, 1994)

It should be realised that no floating structures exist that are only reflective or only dissipative. Distinction is only made to make understanding of the physics easier.

The main effect of reflective structures is to reflect incoming waves so that wave energy behind the structure is reduced (see also Figure 2.1). PIANC (1994) describes fixed structures and oscillating structures. Reflective structures can be divided in an infinitely thin screen (no width or  $w = 0$ ) and a body with a certain width ( $w > 0$ ). Examples of reflecting structures are pontoons or floating breakwaters.

Dissipative systems dissipate wave energy through viscous, or turbulent, effects. PIANC (1994) divides the dissipative systems in two types, surface systems and turbulence generators. The dissipative systems influence wave propagation in at least three ways:

- 1 Their mass and inertia induce a first attenuation, as the reflective systems do;
- 2 They form a semi flexible sheet, which tends to follow fluctuation of the water surface. Provided wave lengths are short enough and the rigidity of the structure is high enough so that restoring forces may be important, this sheet will limit surface vertical displacements;
- 3 Their porosity generates drag forces, which contribute to energy losses.

Examples of surface systems are floating breakwaters made of car tyres (Volker et. al. 1979).

Besides the wave damping aspects, mooring forces are considered as important parameters since forces on mooring systems and the floating structure itself are large. Mooring forces are described in Van den Linden (1985) and PIANC (1994).

Brushwood mattresses resemble dissipating surface systems. This has implications to the type of modelling.



### 3 Physical model tests

#### 3.1 Test set-up

##### 3.1.1 Test facility

Physical model tests were carried out in the Delta Flume of Deltares. The flume has a width of 5.0 m, a height of 7.0 m and an overall length of 240 m. In this flume waves can be generated, up to a significant wave height ( $H_s$ ) of 1.5 m.

##### 3.1.2 Coordinate system

In this report, a coordinate system is used as follows:

$X$  = distance from the wave board in neutral position (m)

$Y$  = distance from the western flume wall (m)

##### 3.1.3 General test set-up

The wave board is located at  $X = 0.0$  m. A 1:4 smooth slope is located with the toe at  $X = 180$  m. Three test series were performed. The difference between those test series is the length of the mattresses. An overview is given in Table 3.1.

Table 3.1 Overview test series

	Width of mattress, $w$ (m)
Test Series 200	12 m
Test Series 300	4 m
Test Series 600	No mattress

The mattress of Test Series 200, which is described in Section 3.2, was placed from  $X = 57$  m until  $X = 69$  m. The mattress of Test Series 300, which is described in Section 3.2, was placed from  $X = 65$  m until  $X = 69$  m. Photographs of installing the mattresses are shown in Photo C.1, Photo C.2 and Photo C.3. Wave height meters, as described in Section 3.3, were placed in front ('seaward side') of the mattresses (at  $X_{GHM11} = 44.00$  m,  $X_{GHM12} = 47.11$  m and  $X_{GHM13} = 49.18$  m) and behind ('landward side') the mattresses (at  $X_{WHM1} = 85.00$  m,  $X_{WHM2} = 87.00$  m and  $X_{WHM3} = 88.00$  m). The water level in all test series was  $h = 4.00$  m. An overview of the test set-up is given in Figure 3.1 and Figure B.1.

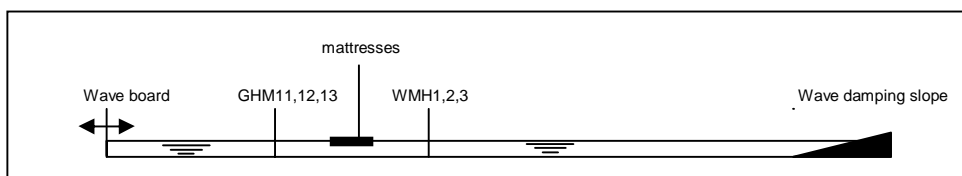


Figure 3.1 Overview test set-up

Waves, as described in Section 3.4, with incident wave energy ( $E_i$ ), were generated at the wave board. The waves travel towards the wave height meters in front of the structure (GHM11, GHM12 and GHM13), and reach the mattress (indicated in Figure B.1 with M1, M2, ..., M6). A part of the wave energy reflects directly ( $E_{r,A}$ ). This reflected wave energy is travelling from the mattress back towards the wave board, which absorbs returning wave energy with the Active Reflection Compensation System. The remainder of the wave energy

$(E_i - E_{r,A})$  is travelling through the mattress, which dissipates a part of this wave energy ( $E_{diss,A}$ ). Resulting wave energy behind the mattress is transmitted wave energy ( $E_{t,A}$ ) which travels towards the wave height meters behind the mattress (WHM1, WHM2, WHM3) and towards the 1:4 smooth concrete slope. The slope reflects a part of this wave energy and resulting wave energy ( $E_{r,B}$ ) travels back in direction of the wave board and passes wave height meters WHM3, WHM2 and WHM1. Then, a part of this energy is re-reflected against the mattress ( $E_{r,C}$ ) and a part of this energy is dissipated in the mattress ( $E_{diss,B}$ ). The resulting transmitted wave energy ( $E_{t,B}$ ) passes the wave height meters GHM13, GHM12 and GHM11 and is absorbed by the wave board. In the analysis it was assumed that re-reflected energy component  $E_{r,C}$  can be neglected. How the several energy components were determined is described in Section 3.3.

## 3.2 Materials

### 3.2.1 Dimensions of mattresses

There is a long tradition in growth, harvesting and braiding of branches of willow trees for specific functions in hydraulic engineering. Braided brushwood mats are used for stabilizing foreshores underwater. However, these mattresses are known to remain buoyant for about two months, which can potentially make them suitable for initiation of floating wetlands. However, the current design should be adapted if buoyancy for longer periods is required. The used mattresses were fabricated by Van Schaik bv. The size of a single mattress was approximately 2.2 m x 4.0 m x 0.45 m ( $B_{str} \times w \times D$ ). The average (wet) mass of one mattress was 367 kg. For Test Series 200, six mattress elements were used (Photo C4), for Test Series 300, two mattress elements were used (Photo C6). Geometric parameters were determined by hand measurements. An overview of dimensions of the mattresses is given in Table A.4, Figure B.1 and Figure B.2.

### 3.2.2 Fixation of mattresses

The mattresses were fixed to each other by using strong ropes. In the first trial tests, this was done by connecting the joints that were located at the edges of the mattress element. This is indicated with blue lines in the lower picture of Figure B.2. However, forces on the ropes were too high and caused severe damage to the mattresses. Therefore, the design was adapted and mattresses were connected using the joints more in the middle of the mattress element. This is shown with the red lines in the lower picture of Figure B.2.

The mattresses were also fixated to the flume wall by ropes. In the first trial tests, the ropes were attached to the joints at the seaward side (side of waveboard) of the mattresses. This is indicated with the blue line in the lower picture of Figure B.2. However, this also resulted in damage to the mattresses. Therefore, ropes were attached to other joints as indicated with the red lines in the lower picture of Figure B.2.

## 3.3 Instrumentation: wave measurements

Wave characteristics were measured by means of three wave gauges in front of the mattresses and three wave gauges behind the mattresses. The location of the wave gauges is given in Table A.3. Wave gauges at the seaward side of the mattresses (GHM11, GHM12 and GHM13) are so-called mechanical wave-followers and they measure surface elevation of the water at a fixed location. Wave gauges at the landward side of the mattresses (WHM1, WHM2 and WHM3) are a pair of vertical wires at a fixed location. They determine surface elevation by measuring electrical resistance between the wires, which is a function of the water level.

To separate incident and reflected waves a cross-correlation technique was used as described by Mansard and Funke (1980). Signals from a set of three wave gauges were used to determine the following wave characteristics:

$H_s = H_{m0}$	significant wave height based on wave spectrum (m)
$T_p$	peak wave period (s)
$N$	number of waves (-)
$s_{o,p}$	deepwater wave steepness $s_{o,p} = \frac{2\pi H_{s,i,1}}{gT_p^2}$ (-)
$C_r$	reflection coefficient (-)
$C_t$	transmission coefficient (-)
$C_{diss}$	dissipation coefficient (-)
$\alpha$	ratio between the dissipated and reflected energy $\alpha = \frac{E_{diss}}{E_r}$ (-)
$p$	percentage of energy (%)

where the following indices are used:

1	location: at seaward side of mattresses (GHM 11, 12, 13)
2	location: at landward side of mattresses (WHM 1, 2, 3)
r	reflected wave
rr	re-reflected wave
i	incident wave
A	wave travelling from wave board through mattress towards slope
B	wave travelling from slope through mattress towards wave board
C	wave re-reflected against landward side of mattresses and travelling from mattresses towards slope

Example:  $H_{s,i,1}$  is the significant incident wave height at the seaward side of the mattresses (GHM11, GHM12 and GHM13)

Energy of waves is partly reflected by the structure ( $E_{r,A}$ ), partly dissipated ( $E_{diss,A}$ ) and partly transmitted ( $E_{t,A}$ ). How this is determined is described in Appendix E and summarized in Figure 3.2.

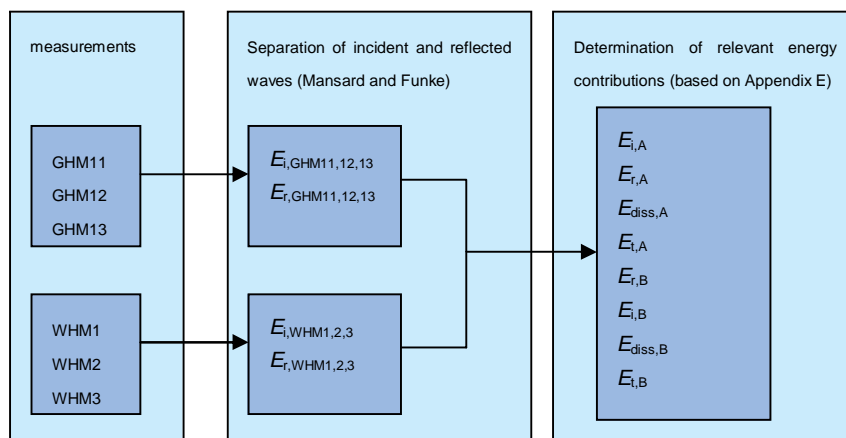


Figure 3.2 Schematisation of determination of the wave energy components



### 3.4 Hydraulic conditions and test programme

For all test-runs, irregular waves (JONSWAP spectrum with a peak enhancement factor of  $\gamma = 3.3$ ) were used. A test-run consisted of around  $N = 1000$  waves. Variation between test-runs are realised by changing significant wave height ( $H_s$ ) and / or wave steepness ( $s_{o,p}$ ). The water depth was  $h = 4.0$  m during all tests. An overview of target wave conditions is given in Table 3.2, Table 3.3 and Table 3.4.

Table 3.2 Overview of wave conditions (target values) for test series T200 ( $w = 12$  m)

	$s_{o,p} = 0.02$	$s_{o,p} = 0.03$	$s_{o,p} = 0.04$
$H_s = 0.20$ m	-	-	T201
$H_s = 0.40$ m	T204	T205	T202
$H_s = 0.60$ m	-	-	T203

Table 3.3 Overview of wave conditions (target values) for test series T300 ( $w = 4$  m)

	$s_{o,p} = 0.02$	$s_{o,p} = 0.03$	$s_{o,p} = 0.04$
$H_s = 0.20$ m	-	T308	T301
$H_s = 0.40$ m	-	T305	T302
$H_s = 0.60$ m	-	-	-

Table 3.4 Overview of wave conditions (target values) for test series T600 (no mattresses)

	$s_{o,p} = 0.02$	$s_{o,p} = 0.03$	$s_{o,p} = 0.04$
$H_s = 0.20$ m	-	-	T601
$H_s = 0.40$ m	-	-	-
$H_s = 0.60$ m	-	-	T603

The test programme with measured wave conditions is given in Table A.1.

### 3.5 Description and visual observation

#### 3.5.1 Test Series 200 ( $w = 12$ m)

During the first trial tests, severe damage to the mattresses was observed. Adaptations as described in Section 3.2.2 were applied to avoid more damage to the mattresses. Due to the damage, willow branches at the landward side of mattresses M1, M2, M3 and M4 (see Figure B.2 of Appendix B) came out of the structure. During following test-runs, these branches were still trapped in between mattresses as can be seen in Appendix C (Photo C.7).

It was clearly visible that individual mattresses could move independently from each other in a vertical direction (the mattresses together cannot be considered as one 'stiff' element). No significant bending of a single mattress was observed.

During the test-runs with steeper waves some wave breaking at the seaward side of the mattresses was observed.

It was visually observed that a wave that rolled into the mattresses resulted in some turbulence. No reflection of waves against the mattress was visually observed. For tests with shorter waves, it could clearly be seen that the transmitted wave height was significantly lower than the incident wave height. The wave crest was clearly a straight line and perpendicular to the flume wall. No 'side effects' due to the open area between the mattresses and the flume wall were visible. The transmitted waves broke as plunging waves

on the 1:4 smooth concrete slope. No reflecting wave energy from the slope was visually observed.

### 3.5.2 Test Series 300 ( $w = 4$ m)

Test Series 300 was performed with two individual mattresses resulting from Test Series 200. (Photo C.6). The loose branches as describes in Section 3.5.1 were not trapped in between the individual mattresses anymore and came loose, as can be seen in Photo C.8.

A wave that rolled into a mattress resulted visibly in turbulence. The transmitted wave height was lower than the incident wave height although this was less intense than in Test Series T200. All other aspects, such as wave breaking at the seaward side of the mattress, perpendicularity of the wave crest, side effects and reflection were the same as for Test Series T200.

### 3.5.3 Test Series 600 (no mattresses)

Some wave breaking (white capping) was observed during Test Series T600.

## 3.6 Results: wave measurements

An overview of measured wave conditions is given in Table A.1. Derived transmission, dissipation and reflection coefficients as described in Appendix E are given in Table A.2. Wave height exceedance curves and energy density spectra are given in Appendix D.



## 4 Analysis

### 4.1 Wave height exceedance curves and energy density spectra

Wave height exceedance curves and wave energy density spectra of all test-runs are given in Appendix D. In general these curves are used to determine distribution of occurring wave heights and to detect outliers. Shown curves all show similar patterns that resemble natural wave fields. In the following analysis, a comparison between three test-runs where significant wave height ( $H_s$ ) is the same but where wave steepness ( $s_{o,p}$ ) differs will be made based on energy density spectra. Energy density spectra of Test T204 ( $s_{o,p} = 0.02$ ), Test T205 ( $s_{o,p} = 0.03$ ) and Test T202 ( $s_{o,p} = 0.04$ ) are displayed in Figure 4.1, Figure 4.2 and Figure 4.3.

Figure 4.1 ( $s_{o,p} = 0.02$ , relatively long waves) shows that the wave spectrum at seaward side and landward side of the mattress is almost the same. Some reduction occurred at higher frequencies, approximately at  $f > 0.3$  Hz. In Figure 4.3 ( $s_{o,p} = 0.04$ , relatively short waves) it can be seen that the wave energy is reduced over almost the whole frequency domain (lower limit of frequency domain is approximately  $f = 0.3$  Hz). In Figure 4.2 ( $s_{o,p} = 0.03$ ) a reduction of wave energy can be seen as well. Also in this graph reduction starts at approximately  $f = 0.3$  Hz.

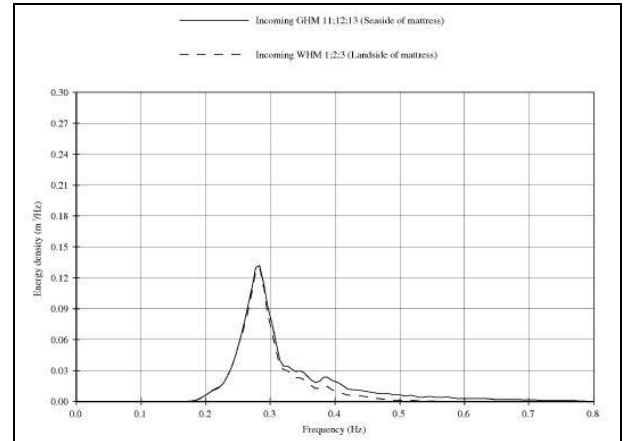


Figure 4.1 Wave spectra Test T204 ( $s_{o,p} = 0.02$ ,  $H_s = 0.4$  m)

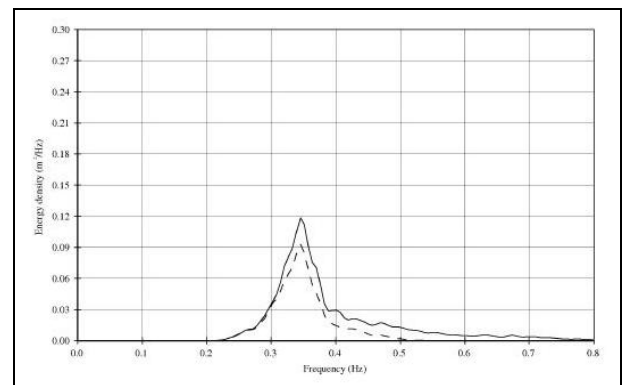


Figure 4.2 Wave spectra Test T205 ( $s_{o,p} = 0.03$ ,  $H_s = 0.4$  m)

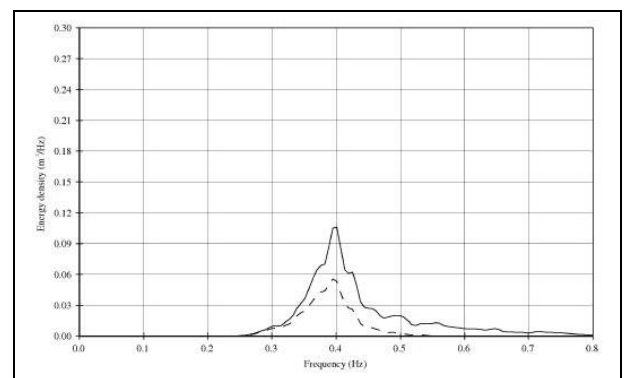


Figure 4.3 Wave spectra Test T202 ( $s_{o,p} = 0.04$ ,  $H_s = 0.4$  m)

Test-runs with same hydraulic conditions but different mattress lengths are compared as well. An overview of comparable test runs is given in Table 4.1.

Table 4.1 Overview of comparison of wave height exceedance curves and energy spectra

Test	Figure	Wave height $H_s$ (m)	Wave steepness $s_{o,p}$ (-)	Mattress length $w$ (m)
T201 vs. T301	Fig. D.1 / D.6	0.20	0.04	12 / 4
T202 vs. T302	Fig. D.2 / D.7	0.40	0.04	12 / 4
T205 vs. T305	Fig. D.4 / D.8	0.40	0.03	12 / 4

As an example, Test T202 ( $w = 12$  m) and Test T302 ( $w = 4$  m) are shown in Figure 4.4 and Figure 4.5.

Mattresses with a length ( $w$ ) of 12 m influence the wave spectrum at a frequency of approximately  $f > 0.3$  Hz, the mattresses with a length of  $w = 4$  m influence the wave spectrum at a higher frequency of around  $f > 0.35$  Hz.

From the above it can be concluded that the length of the mattresses  $w$  and the length of the waves  $L$ , have a significant influence on the wave damping. A shorter wave is dissipated more than a longer wave. A longer mattress will dissipate more wave energy than a shorter mattress.

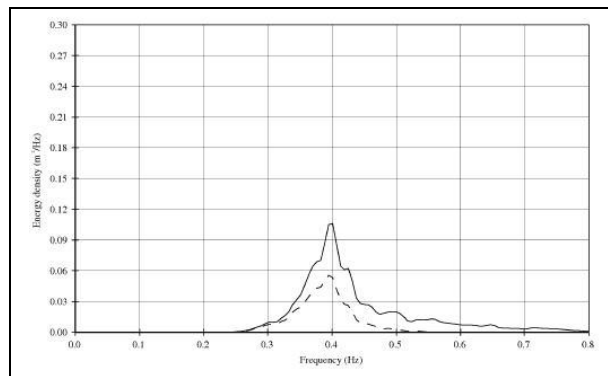


Figure 4.4 Wave spectra Test T202 ( $H_s = 0.4$  m,  $w = 12$  m)

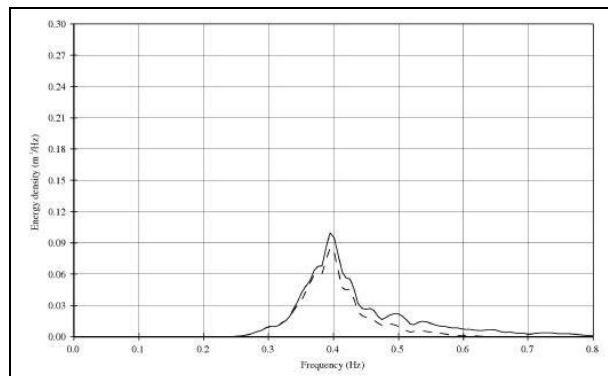


Figure 4.5 Wave spectra Test T302 ( $H_s = 0.4$  m,  $w = 4$  m)

## 4.2 Transmission coefficient

Transmission coefficient  $C_t$  as function of significant wave height  $H_{m0}$  is displayed in Figure 4.6. Transmission coefficient  $C_t$  as function of significant wave height  $H_{m0}$  shows scatter for five measurement points around  $H_s \approx 0.4$  m. Differences between these specific tests is difference in length of mattress  $w$  (4 m; 12 m) and wave steepness  $s_{o,p}$  (0.02; 0.03; 0.04) or wave length. To account for length of mattress and wavelength, transmission coefficient  $C_t$  is plotted as function of ratio of length of mattress and local wavelength  $w/L_p$  in right panel of Figure 4.6. For each single mattress length, scatter decreased compared to the left panel of Figure 4.6.

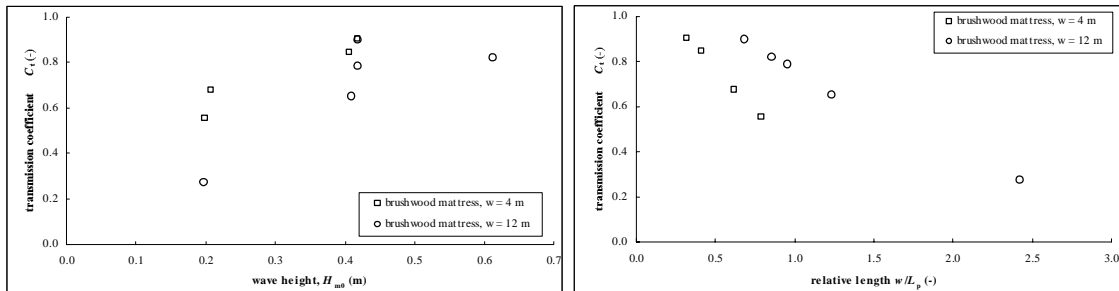


Figure 4.6 Transmission coefficient  $C_t$  as function of  $H_{m0}$  and as function of relative mattress length  $w/L_p$

Between Test Series T200 ( $w = 12$  m) and Test Series T300 ( $w = 4$  m) a difference in transmission coefficient  $C_t$  was found (see right panel of Figure 4.6). This is firstly explained by differences length of mattress  $w$ . However, when dimensionless length of mattress  $w/L_p$  is kept constant, transmission coefficient  $C_t$  between Test Series T200 and Test Series T300 still differ. This is explained by the relative thickness of mattresses. Both mattresses of 4 m and 12 m have a thickness under water  $d$  of around 0.30 m. This implies that mattresses of Test Series T300 ( $w = 4$  m) are relatively three times thicker than those of Test Series T200 ( $w = 12$  m). It is very likely that, for each given value of  $w/L_p$ , a relatively thicker mattress will dissipate more wave energy. This explains the transmission coefficient of Test Series T300, which is lower than the transmission coefficient of Test Series T200.

To compensate for thickness of mattress, relative thickness should be included in the dimensionless parameter displayed on horizontal axis of Figure 4.6. This is quite complicated due to the non-uniform distribution of the wave energy over the water depth. With relatively shallow water ( $kh \ll 1$  where  $k$  is wave number ( $k = 2\pi/L_p$ )), wave energy is uniformly distributed over water depth. With relatively deep water ( $kh > 1$ ), this is not the case, see Figure 4.7.

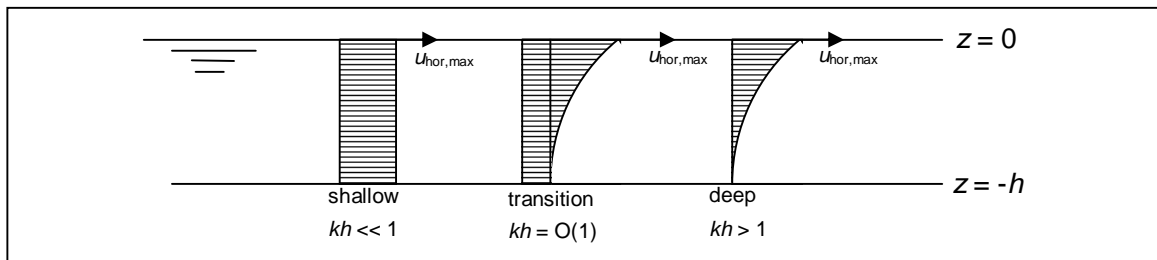


Figure 4.7 Vertical energy distribution for shallow and deep water

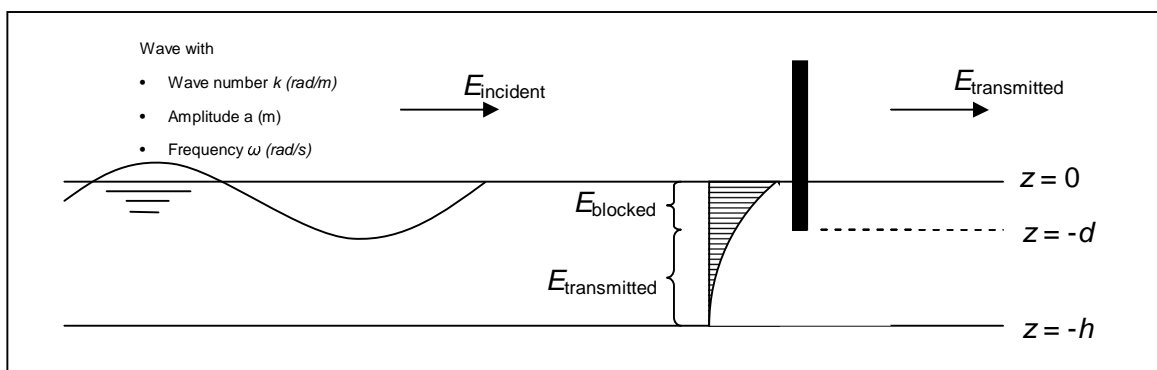


Figure 4.8 Schematisation of object blocking a wave

Attenuation of wave energy as a function of ratio of water depth to wavelength  $h/L_p$  and ratio of water depth to protrusion depth of mattress  $d/h$  is shown in the left panel of Figure 4.9. A theoretical derivation of this figure is given in Appendix F. Ratio of blocked wave energy is noted with  $\chi_{BL}$ , ratio of energy passing underneath the structure is noted with  $\chi_t$ .

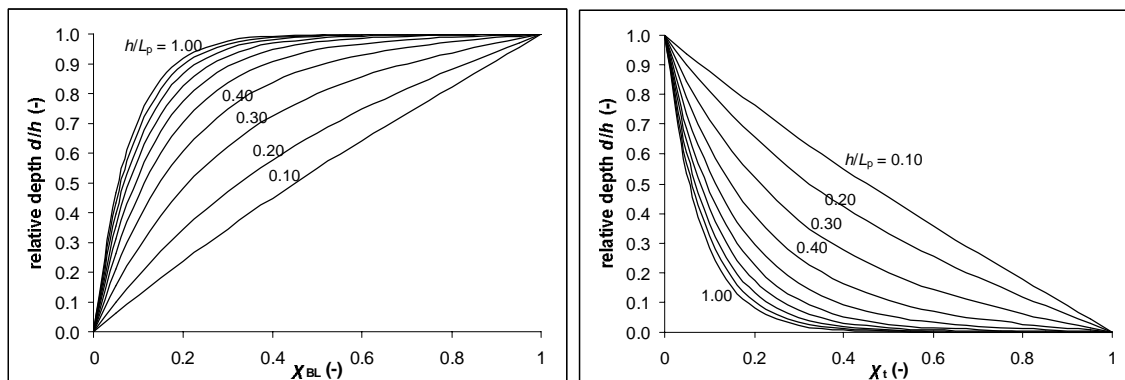


Figure 4.9 Effect of wave and structure depth (derivation in Appendix F)

Ratio of blocked energy  $\chi_{BL}$  can be expressed by:

$$\chi_{BL} = \frac{\sinh 2kh - \sinh 2k(h-d) + 2kd}{\sinh 2kh + 2kh} \quad (4.1)$$

Where

- $k$  = wave number ( $= 2\pi/L_p$ ) [rad/m]
- $h$  = water depth at structure [m]
- $d$  = protrusion depth of structure [m]
- $\chi_{BL}$  = ratio of energy at structure [-]

Eq. (4.1) is derived in Appendix F. This schematization assumes no vertical movement of tested mattresses. Although this is not the case for this test set-up, it might serve as a good first guess. With Eq. (4.1),  $\chi_{BL}$  is determined for each individual test and presented in Figure 4.10. Values of  $h/L_p$ ,  $d/h$  and  $\chi_{BL}$  are given in Table A.1.

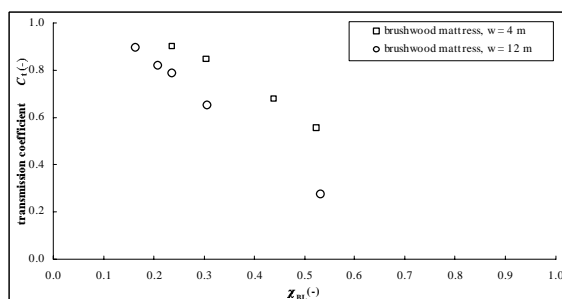


Figure 4.10 Transmission coefficient as function of blocked wave energy  $\chi_{BL}$

Now it is possible to correct dimensionless parameter  $w/L_p$  with ratio of blocked wave energy  $\chi_{BL}$ , which is shown in Figure 4.11. It can be seen that scatter of data is very low.



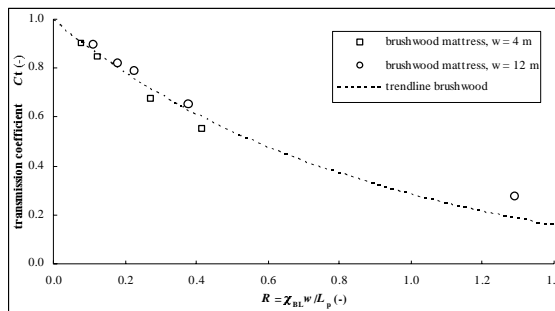


Figure 4.11 Transmission coefficient  $C_t$  as function of dimensionless parameter  $(w/L_p)X_{BL}$

### 4.3 Prediction of transmission, reflection and dissipation coefficient

In Figure B.3, Figure B.4 and Figure B.5, it can be seen that reflection coefficient  $C_r$  is approximately constant for all tests. Therefore, reflection coefficient  $C_r$  is defined by:

$$C_r = 0.1 \tag{4.2}$$

In top panels of Figure B.3, Figure B.4 and Figure B.5, dissipation coefficient  $C_{diss,A}$  is shown. Data collapse of dissipation coefficient  $C_{diss,A}$  significantly increases when using dimensionless parameter  $(w/L_p)X_{BL}$ . Based on analysis given in Appendix G, Eq. (4.3) is used as a starting point for determination a fitting line:

$$C_{diss} = \sqrt{1 - e^{-fx}} \tag{4.3}$$

with  $x$  chosen as:

$$x = X_{BL} \frac{w}{L_p} \tag{4.4}$$

gives

$$C_{diss} = \sqrt{1 - e^{-f X_{BL} \frac{w}{L_p}}} \tag{4.5}$$

$f$  is chosen as 2.4 which gives the best fit. Result of measured dissipation coefficient and trend line based on Eq. (4.5) and  $f = 2.4$  is given in Figure 4.12.

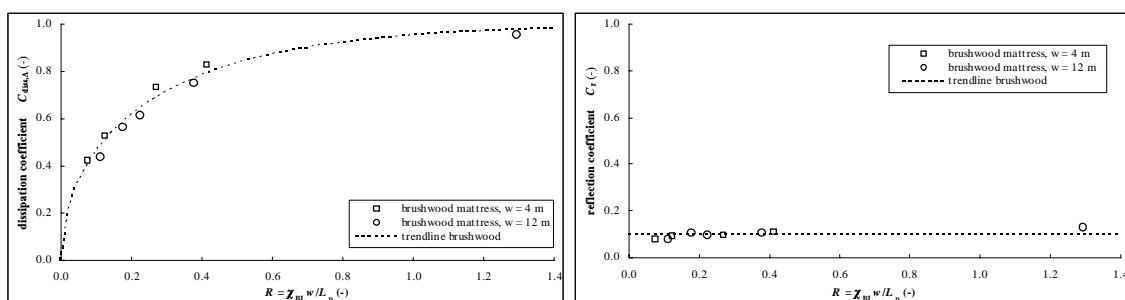


Figure 4.12 Measured dissipation and reflection coefficients and derived trend line

Now transmission coefficient  $C_t$  can be derived by

$$C_t = \sqrt{1 - C_{diss}^2 - C_r^2} \quad (4.6)$$

Rewriting gives:

$$C_t = \sqrt{e^{-f \chi_{BL} \frac{w}{L_p}} - C_r^2} \quad (4.7)$$

Resulting trend line based on Eq. (4.7) with  $f = 2.4$  and  $C_r = 0.1$  is given in Figure 4.11.

#### 4.4 Summary prediction model

To predict wave transmission through brushwood mattresses, following equations are suggested:

Wave number  $k = \frac{2\pi}{L_p}$  (4.8)

Blocked energy ratio  $\chi_{BL} = \frac{\sinh 2kh - \sinh 2k(h-d) + 2kd}{\sinh 2kh + 2kh}$  (4.9)

Dissipation coefficient  $C_{diss} = \sqrt{1 - e^{-f \chi_{BL} \frac{w}{L_p}}}$  with  $f = 2.4$  (4.10)

Reflection coefficient  $C_r = 0.1$  (4.11)

Transmission coefficient  $C_t = \sqrt{e^{-f \chi_{BL} \frac{w}{L_p}} - C_r^2}$  (4.12)

Transmitted wave height  $H_{m0,t} = C_t H_{m0,i}$  (4.13)

With

$C_{diss}$	=	dissipation coefficient	[-]
$C_r$	=	reflection coefficient	[-]
$C_t$	=	transmission coefficient	[-]
$d$	=	water depth	[m]
$f$	=	coefficient, = 2.4	[-]
$h$	=	depth of structure under water	[m]
$H_{m0,t}$	=	transmitted significant wave height	[m]
$H_{m0,i}$	=	incident significant wave height	[m]
$k$	=	wave number	[rad/m]
$L_p$	=	local peak wave length	[m]
$w$	=	length of structure	[m]
$\chi_{BL}$	=	wave energy blocking ratio	[-]

First, wave number  $k$  is determined with use of Eq. (4.8) which served as input for determination of blocking wave energy ratio parameter  $\chi_{BL}$  with use of Eq. (4.9). Now transmission coefficient  $C_t$  and transmitted wave height  $H_{m0,t}$  can be determined using Eq. (4.12) and Eq. (4.13).

#### 4.5 Restrictions of wave damping prediction model

In previous sections a calculation method is given. This method is based on the assumption that drag forces generated by porosity of structure, which contribute to energy losses wave, cause wave damping (dissipative system as described in Chapter 2).

When using this prediction model one should realize that the theoretical model as described is based on empirical data where:

1. Anchoring / mooring did not play a significant role with respect to wave damping. If anchors will be applied, actual wave damping effect is assumed to be higher than the model predicts. Anchor forces might, however, also lead to more damage to the mattresses.
2. There was no significant stiffness in the mattresses implying that the mattresses had no significant restoring force. Restoring forces might increase wave damping characteristics. If restoring forces are significant, (e.g. mattresses are stiffly connected or one large mattress was used) actual damping wave damping effect might be higher than the model predicts.
3. Porosity did not significantly change during test series. In actual situation porosity characteristics might change due to degradation or biological activity. It is not clear what influence of porosity is with respect to wave damping characteristics.
4. Data has a limited range. The range of tested parameters is given in Table 4.2. Relevant dimensionless parameters are given in Table 4.3.

Table 4.2 Range of tested conditions

Parameter	range
water depth	$h = 4.00$ m
mattress depth under water	$d = 0.3$ m
mattress length	$4$ m $\leq w \leq 12$ m
wave length	$5.0 \leq L_p \leq 17.6$
significant wave height	$0.20 \leq H_s \leq 0.60$ m

Table 4.3 Range of tested conditions (dimensionless)

Parameter	range
ratio mattress length and wave length	$0.3 \leq w/L_p \leq 2.4$
ratio mattress depth and water depth	$d/h = 0.075$
ratio water depth and wave length	$0.2 \leq h/L_p \leq 0.8$
wave steepness based on deep water peak period	$0.021 \leq s_{o,p} \leq 0.042$
wave steepness based on local water peak period	$0.024 \leq s_p \leq 0.044$
ratio blocked wave energy	$0.2 \leq \chi_{BL} \leq 0.5$

#### 4.6 Example of using prediction model

An example, which illustrates how to use the prediction method as given in this report, is given below. Required hydraulic and geometric input conditions are given in Table 4.4 and Table 4.5. Results and warnings are given in Table 4.6 and Table 4.7.

Table 4.4 Hydraulic conditions of test case

parameter	value
water depth	$h$ 6.0 m
significant wave height	$H_{m0}$ 1.0 m
local peak wave length	$L_p$ 33.3 m

Table 4.5 Mattress conditions of tests case

parameter		value
thickness (under water)	$d$	0.60 m
length of mattress	$w$	100 m

Table 4.6 Results of test case

parameter		equation	result
wave number	$k$	(4.8)	0.19 rad/m
energy blocking ratio	$\chi_{BL}$	(4.9)	0.173
transmission coefficient	$C_t$	(4.12)	0.53
transmitted wave height	$H_{mo,tr}$	(4.13)	0.53 m

Table 4.7 Warnings given for test case

parameter		warning
ratio mattress length and wave length	$w/L_p$	Outside range of tested conditions
ratio mattress depth and water depth	$d/h$	Outside range of tested conditions
ratio water depth and wave length	$h/L_p$	Outside range of tested conditions
Ratio blocked wave energy	$\chi_{BL}$	Outside range of tested conditions

Appendix H gives an impression of the developed calculation tool.

#### 4.7 Strength aspects

Focus of this research project was on wave damping aspects of brushwood mattresses. However, it was observed that some damage occurred to brushwood mattresses during the test program. When constructing a prototype mattress, attention should be paid to constructional details of the mattress.

To keep the mattress at its place anchorage is required. This anchorage will give large forces on the mattresses. For several types of floating breakwaters this anchor forces are very high and might lead to damage.

## 5 Conclusions and recommendations

### 5.1 Conclusions

To obtain a first quantification of wave damping properties of floating wetlands a prediction tool based on large-scale flume experiments and based on a theoretical approach is developed. Mattress characteristics (depth under water  $d$  and mattress length  $w$ ) and hydraulic characteristics (water depth  $h$  and wavelength  $L_p$ ) are identified as important parameters with respect to wave damping. Results are summarized in Figure 5.1 and Eq. (5.1) and Eq. (5.2).

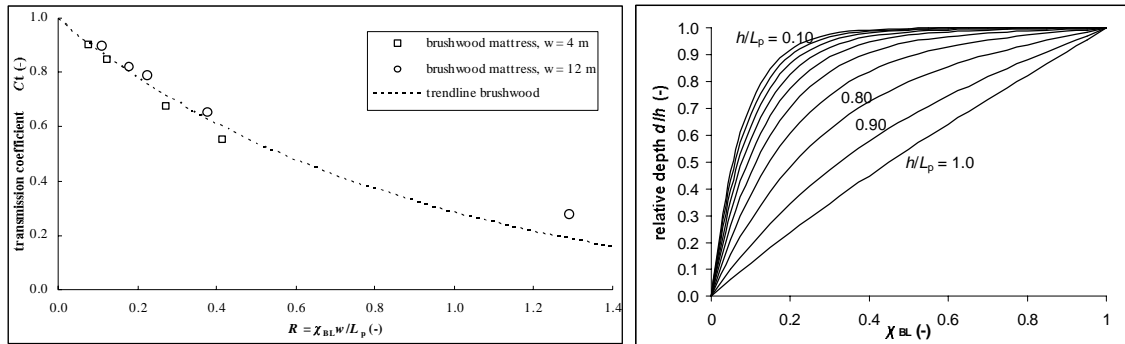


Figure 5.1 Transmission coefficient  $C_t$  as function of mattress length  $w$ , wave length  $L_p$  and ratio of blocked wave energy  $\chi_{BL}$

$$\chi_{BL}(k, h, d) = \frac{\sinh 2kh - \sinh 2k(h-d) + 2kd}{\sinh 2kh + 2kh} \quad (5.1)$$

$$C_t = \sqrt{e^{-f \chi_{BL} \frac{w}{L_p}} - C_r^2} \quad (5.2)$$

Where  $f = 2.4$  is empirical derived and reflection coefficient  $C_r = 0.1$

Measured transmission coefficient  $C_t$  varied between 0.25 and 0.90. Tested conditions are summarized in Table 4.2 and Table 4.3 and indicated the validation range of the prediction model.

Several theoretical wave-damping mechanisms, such as reflection, restoring forces due to stiffness of mattress and turbulence are discussed. For all tests, reflection coefficient  $C_r$  was approximately 0.1. It is very likely that significant wave-damping physical process in this test set-up is mainly determined by turbulence and less by reflections or restoring forces (no significant bending of mattress as a whole was possible due to type of connection of individual elements).

### 5.2 Recommendations

#### 5.2.1 Wave damping characteristics

A first estimate of wave damping characteristics can be made based on results of this study. However, caution should be taken when up scaling the results to field situations. It is strongly recommended to test a larger range (longer elements and larger waves, other water depths)

in a large-scale flume before applying this in a prototype situation. (example: physical experiment with a mattress length ( $w$ ) of 50 m and a depth under water ( $d$ ) of 0.60 m with wave heights between  $H_s = 0.40$  m and  $H_s = 1.30$  m, with varying depths).

## 5.2.2 Other engineering aspects: strength and anchorage

The focus of this study was primarily on wave damping characteristics. However, during testing, several problems with respect to strength of mattresses occurred. Although this could be solved relatively easily with tie-wraps or steel rope, it is strongly recommended to perform an additional analysis with respect to strength of mattresses and test new designs in physical models before applying them to the field.

When applying floating breakwaters, anchorage requires special attention. Anchorage is relevant with respect to wave damping. It is very likely that this will improve wave damping characteristics but might also give severe damage to mattresses. It is recommended to study this aspect (desk study / physical model) before applying brushwood mattresses on large scales in the field.

## 6 References

- Lochner, R. Faber, O. and Penny, W., *The Civil Engineer in War, Vol. 2, Docks and harbours*, The institution of Civil engineers, London, England, 1948, pp, 256-290
- Mansard, E.P.D. and Funke, E.R., 1980, *The measurement of incident waves and reflected spectra using a least square method*, 17<sup>th</sup> Int. Conf. of Coastal Engineering, Sydney.
- PIANC, 1994, *Floating Breakwaters, A practical Guide for design and construction*", report of working group no. 13 of the permanent Technical Committee II, supplement to bulletin No. 85 (1994), ISBN 2-87223-052-1
- Van der Linden, M., 1985, *Golfdempende constructies (in Dutch)*, Delftse Universitaire Pers, ISBN 90-6275-263-2 SISO 699.2 UDC 627-235
- Volker, W., Harms, M. 1979, *Design criteria for floating tire breakwaters*, Journal of the waterway port coastal and ocean division, proceedings of the American Society of Civil Engineers, Vol. 105, No. WW2, May 1979





## A Tables

*Table A.1 Measured wave conditions*

*Table A.2 Reflection, transmission and dissipation coefficients*

*Table A.3 Coordinates of all objects*

*Table A.4 Characteristics of mattresses*



Table A.1: Measured wave conditions

Test	basic parameters			WHM's seaward side of mattresses (GHM 11, 12, 13)								WHM's landward side of mattresses (WHM 1, 2, 3)					dimensionless parameters					
	water depth	structural length	structural depth	incident wave height	incident wave period	deep water wave length	wave length	wave number	incident wave steepness	nr. of incident waves	reflected wave height	incident wave height	incident wave period	incident wave steepness	nr. of incident waves	reflected wave height	dim. width	dim. wave length	relative depth of structure	energy blocking ratio	energy transmission ratio	dimensionless parameter
	$h$ (m)	$w$ (m)	$d$ (m)	$H_{s,i,1}$ (m)	$T_{p,i,1}$ (s)	$L_{o,p,i}$ (m)	$L_{p,i}$ (m)	$k$ (m)	$s_{o,i,1}$ (-)	$N_{i,1}$ (-)	$H_{s,r,1}$ (m)	$H_{s,i,2}$ (m)	$T_{p,i,2}$ (s)	$s_{o,i,2}$ (-)	$N_{i,2}$ (-)	$H_{s,r,2}$ (m)	$w/L_{p,i}$ (-)	$L_{p,i}/h$ (-)	$d/h$ (-)	$X_{BL}$ (-)	$X_{TR}$ (-)	$X_{BL}(w/L_{p,i})$ (-)
T201	4.00	12.0	0.3	0.197	1.78	4.95	4.95	1.27	0.040	984	0.025	0.054	1.95	0.009	856	0.012	2.43	1.24	0.075	0.53	0.47	1.29
T202	4.00	12.0	0.3	0.410	2.51	9.87	9.75	0.64	0.042	1101	0.047	0.267	2.53	0.027	966	0.027	1.23	2.44	0.075	0.31	0.69	0.38
T204	4.00	12.0	0.3	0.419	3.56	19.78	17.61	0.36	0.021	1166	0.050	0.376	3.56	0.019	1058	0.042	0.68	4.40	0.075	0.16	0.84	0.11
T205	4.00	12.0	0.3	0.419	2.89	13.06	12.58	0.50	0.032	1151	0.048	0.329	2.90	0.025	1006	0.033	0.95	3.14	0.075	0.24	0.76	0.22
T203	4.00	12.0	0.3	0.612	3.09	14.89	14.06	0.45	0.041	1162	0.075	0.502	3.09	0.034	1024	0.048	0.85	3.52	0.075	0.21	0.79	0.18
T301	4.00	4.0	0.3	0.199	1.80	5.07	5.06	1.24	0.039	979	0.024	0.110	1.86	0.020	912	0.017	0.79	1.27	0.075	0.52	0.48	0.41
T302	4.00	4.0	0.3	0.406	2.52	9.91	9.79	0.64	0.041	1099	0.047	0.343	2.53	0.034	1003	0.034	0.41	2.45	0.075	0.31	0.69	0.12
T305	4.00	4.0	0.3	0.418	2.88	12.94	12.48	0.50	0.032	1045	0.049	0.377	2.90	0.029	952	0.040	0.32	3.12	0.075	0.24	0.76	0.08
T308	4.00	4.0	0.3	0.207	2.04	6.48	6.47	0.97	0.032	1026	0.023	0.141	2.07	0.021	941	0.016	0.62	1.62	0.075	0.44	0.56	0.27
T601	4.00	0.0	0.0	0.196	1.79	4.99	4.99	1.26	0.039	986	0.024	0.189	1.79	0.038	987	0.020	0.00	1.25	0.000	0.00	1.00	0.00
T603	4.00	0.0	0.0	0.601	3.09	14.86	14.04	0.45	0.040	1148	0.095	0.604	3.08	0.041	1128	0.085	0.00	3.51	0.000	0.00	1.00	0.00

Table A.2: reflection, transmission and dissipation coefficients

	reflection coefficients			transmiss. coeff	dissip. coeff		ratio	from wave board to slope				from slope to wave board			
	reflection coefficient (A)	reflection coefficient (B)	reflection coefficient (C)	transmission coefficient (A)	transmission coefficient (B)	dissipation coefficient (A)	dissipation coefficient (B)	ratio dissipation reflection	reflection A	dissipation A	reflection on slope	breaking on slope	re reflection C	dissipation B	wave board absorption
Test	$C_{r,A}$ (-)	$C_{r,B}$ (-)	$C_{r,C}$ (-)	$C_{t,A}$ (-)	$C_{t,B}$ (-)	$C_{diss,A}$ (-)	$C_{diss,B}$ (-)	$\alpha_A$ (-)	$P_{r,A}$ (%)	$P_{diss,A}$ (%)	$P_{r,slope}$ (%)	$P_{bs,A}$ (%)	$P_{rr,A}$ (%)	$P_{diss,B}$ (%)	$P_{ARC,B}$ (%)
T201	0.13	0.22	0.00	0.27	0.27	0.95	0.96	57.4	2%	91%	0%	7%	0%	92%	8%
T202	0.11	0.10	0.00	0.65	0.65	0.75	0.76	50.0	1%	56%	0%	42%	0%	58%	42%
T204	0.08	0.11	0.00	0.90	0.90	0.43	0.44	30.7	1%	19%	1%	80%	0%	19%	81%
T205	0.10	0.10	0.00	0.79	0.79	0.61	0.62	40.2	1%	37%	1%	61%	0%	38%	62%
T203	0.10	0.10	0.00	0.82	0.82	0.56	0.57	29.1	1%	32%	1%	67%	0%	33%	67%
T301	0.11	0.15	0.00	0.55	0.55	0.83	0.83	55.4	1%	68%	1%	30%	0%	69%	31%
T302	0.09	0.10	0.00	0.84	0.84	0.53	0.54	33.1	1%	28%	1%	71%	0%	29%	71%
T305	0.08	0.11	0.00	0.90	0.90	0.42	0.43	28.6	1%	18%	1%	80%	0%	19%	81%
T308	0.10	0.11	0.00	0.68	0.68	0.73	0.74	55.4	1%	53%	1%	45%	0%	54%	46%
T601	-	-	-	-	-	-	-	-	-	-	-	-	-	-	-
T603	-	-	-	-	-	-	-	-	-	-	-	-	-	-	-

"A" indicates the wave traveling from the wave board through the mattresses towards the slope

"B" indicates the wave traveling from the slope through the mattresses towards the wave board

"C" indicates the reflected wave from the slope that is re-reflected against the landward side of the mattresses and travels towards the slope

Table A.3: Coordinates of all objects

Object	Test Series 200 ( $w = 12\text{ m}$ )		Test Series 300 ( $w = 4\text{ m}$ )		Test Series 600 (No mattress)	
	X (m)	Y (m)	X (m)	Y (m)	X (m)	Y (m)
Wave board	0	0 - 5	0	0 - 5		0 - 5
GHM11	44.00	2.50	44.00	2.50	44.00	2.50
GHM12	47.11	2.50	47.11	2.50	47.11	2.50
GHM13	49.18	2.5	49.18	2.50	49.18	2.50
front of mattress	57	0 - 5	65	0 - 5	-	-
back of mattress	69	0 - 5	69	0 - 5	-	-
WHM1	85.00	0.05	85.00	0.05	85.00	0.05
WHM2	87.00	0.05	87.00	0.05	87.00	0.05
WHM3	88.00	0.05	88.00	0.05	88.00	0.05
slope	180.0	0 - 5	180.0	0 - 5	180	0 - 5

Table A.4 Characteristics of mattresses

parameter		Single mattress	Test Series	
			200	400
number of mattresses	$n$ (-)	1	3 x 2	1 x 2
length	$w$ (m)	4	12	4
width	$B_{\text{str}}$ (m)	2.2	4.4	4.4
height	$D$ (m)	0.44	0.44	0.44
mass (wet)	$m$ (kg)	367	2200	733
height under water	$d$ (m)	0.30	0.30	0.30



## B Figures

*Figure B.1 Overview of test set-up*

*Figure B.2 Detail of mattresses*

*Figure B.3 Transmission, reflection and dissipation coefficient as function of significant wave height  $H_{m0}$*

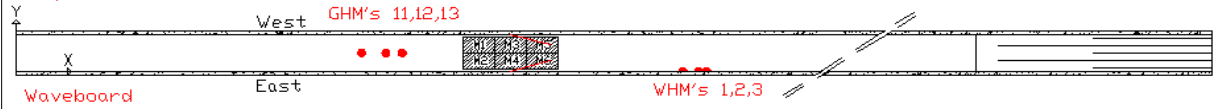
*Figure B.4 Transmission, reflection and dissipation coefficient as function of relative mattress length  $w/L_p$*

*Figure B.5 Transmission, reflection and dissipation coefficient as function of  $(w/L_p)\chi_{BL}$*

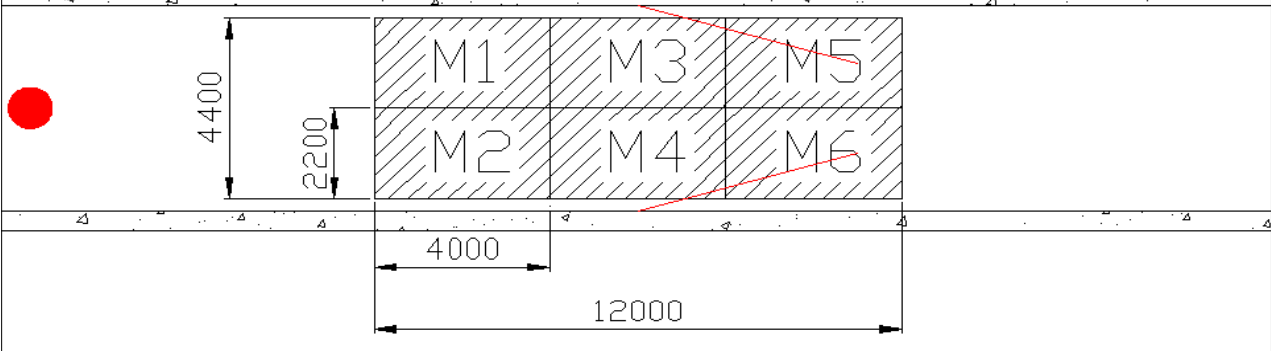
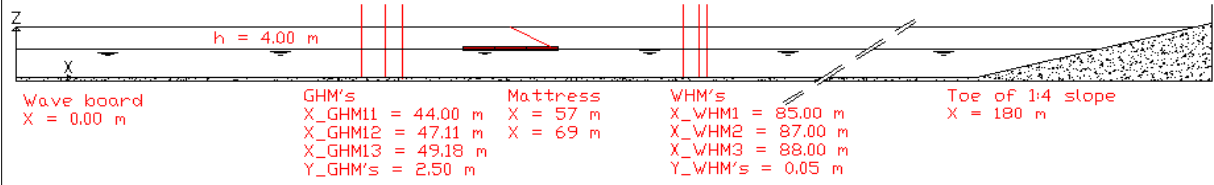




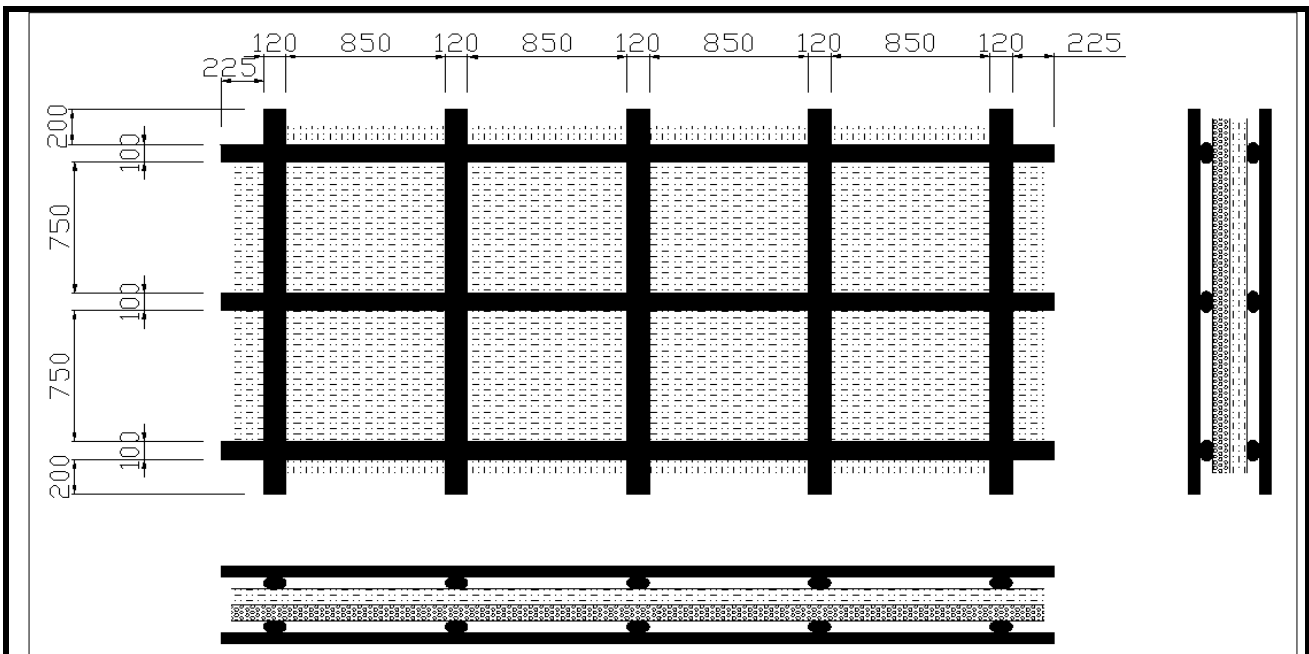
Top view



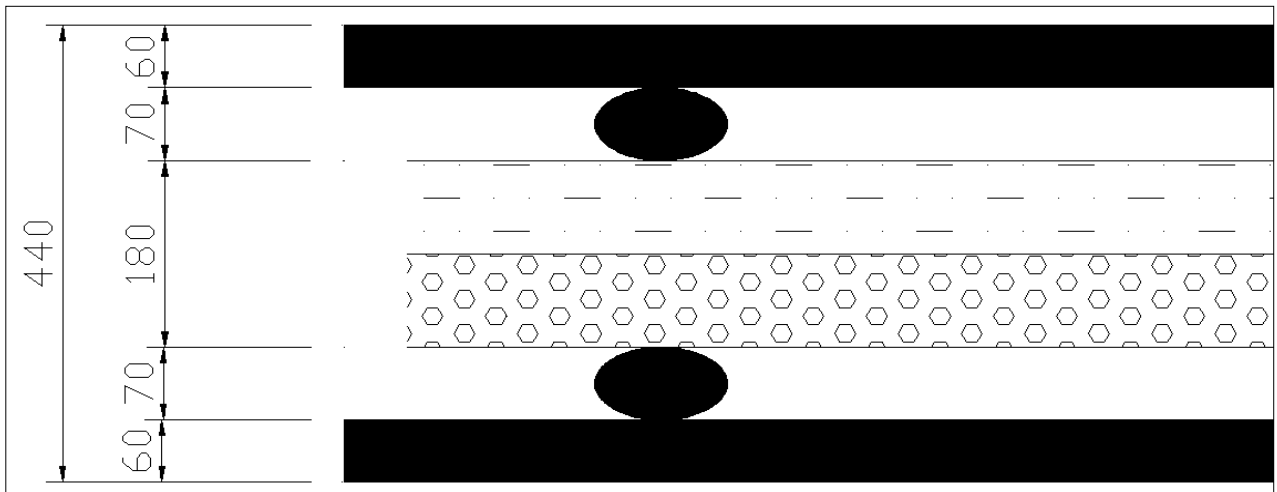
Side view



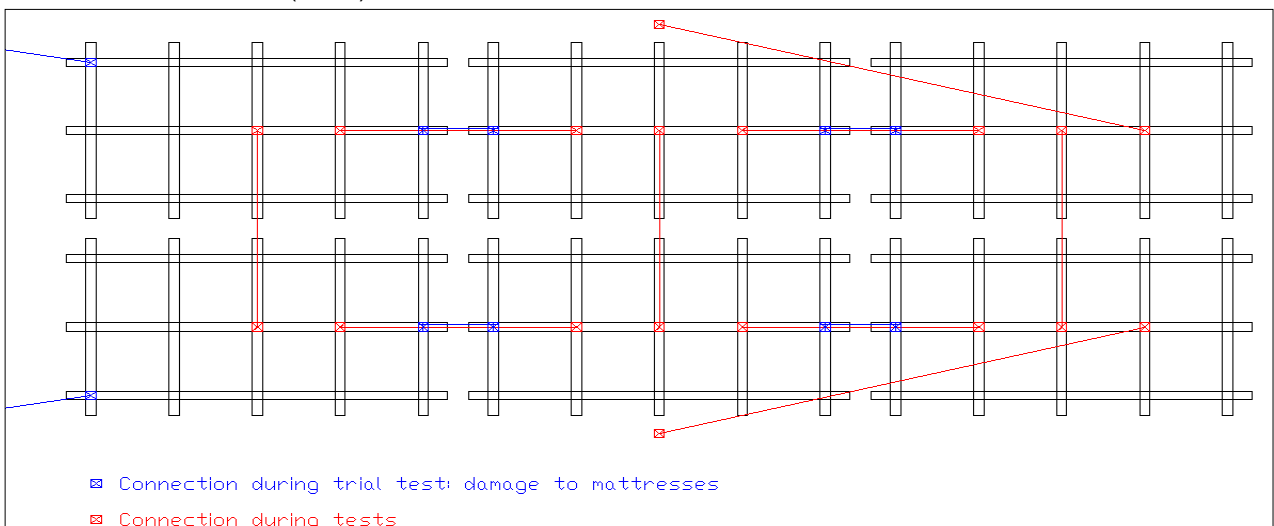
Overview of test set-up



Dimensions of mattresses (overview)



Dimensions of mattresses (detail)



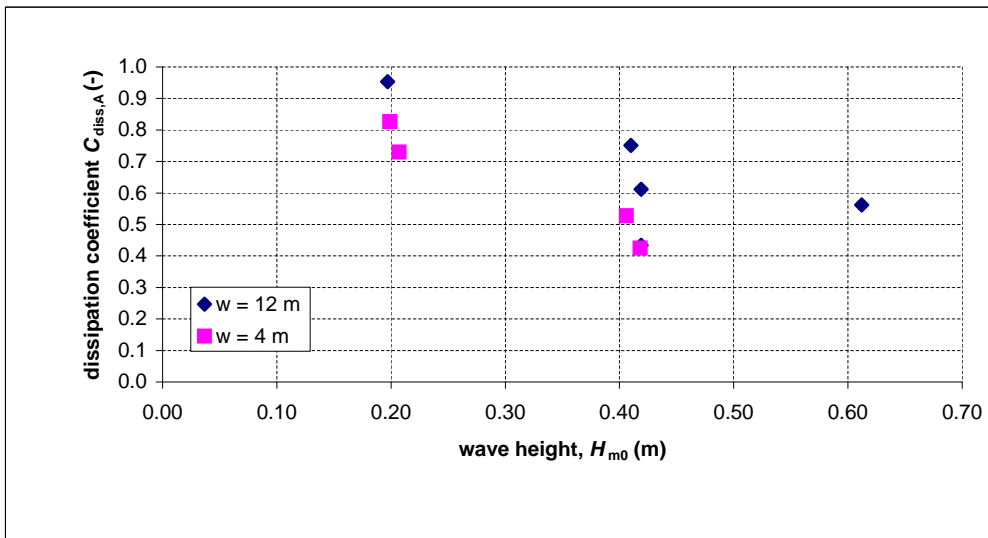
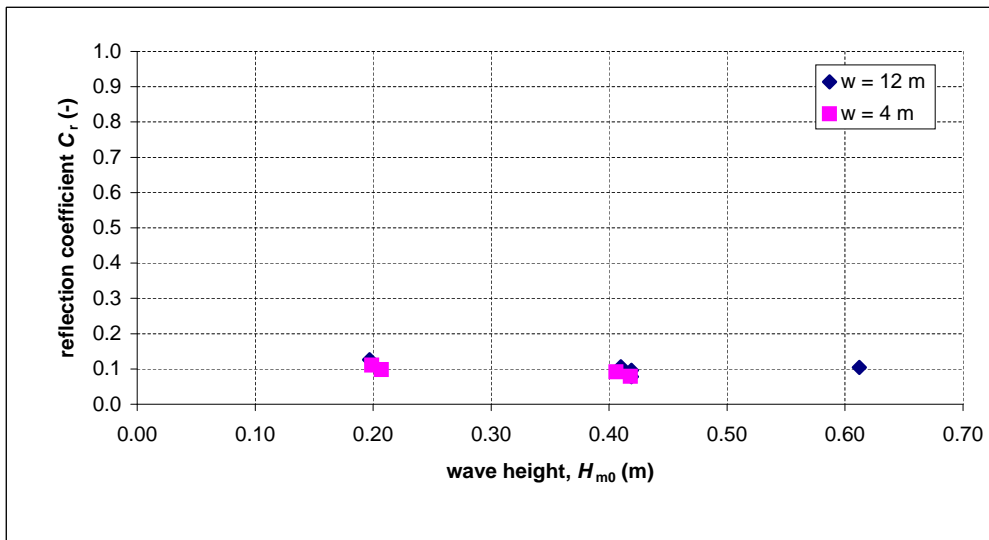
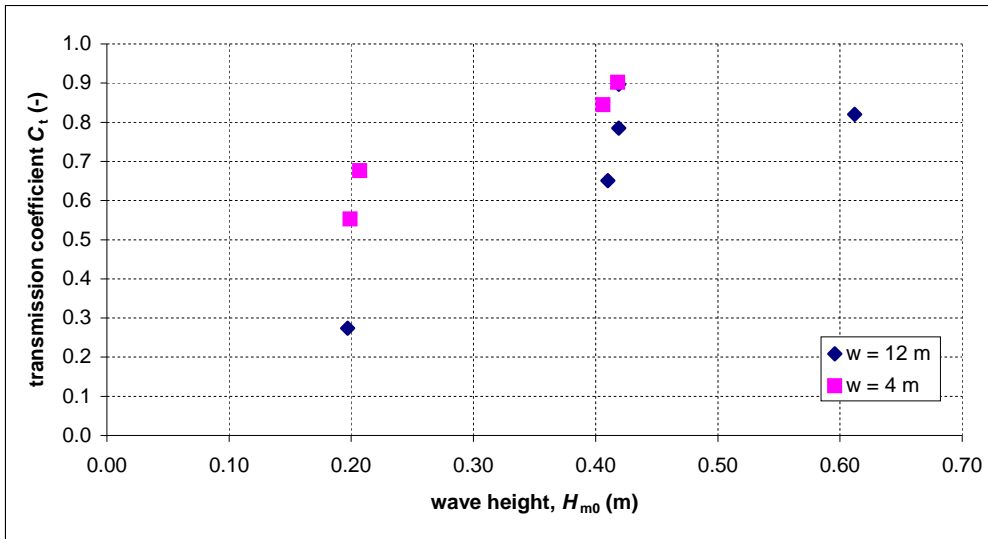
Connection of mattresses with ropes

Detail of mattresses

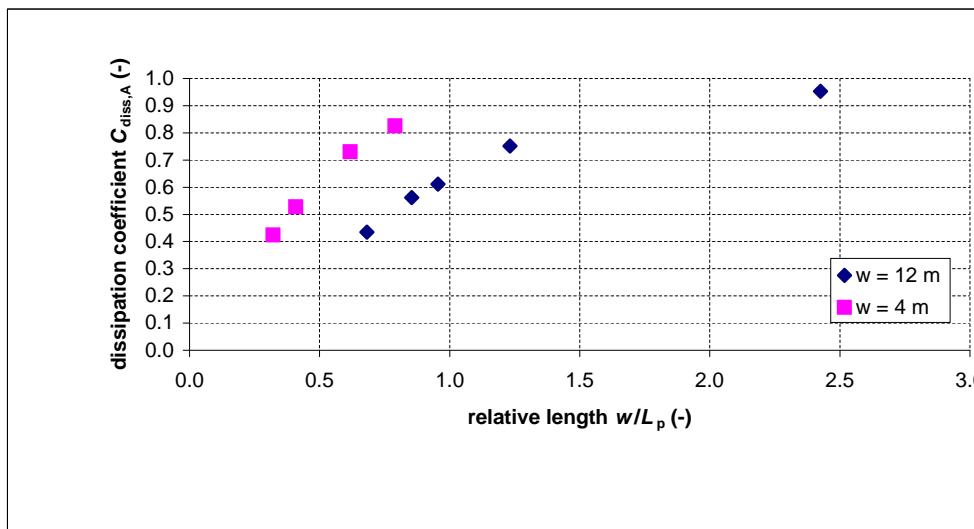
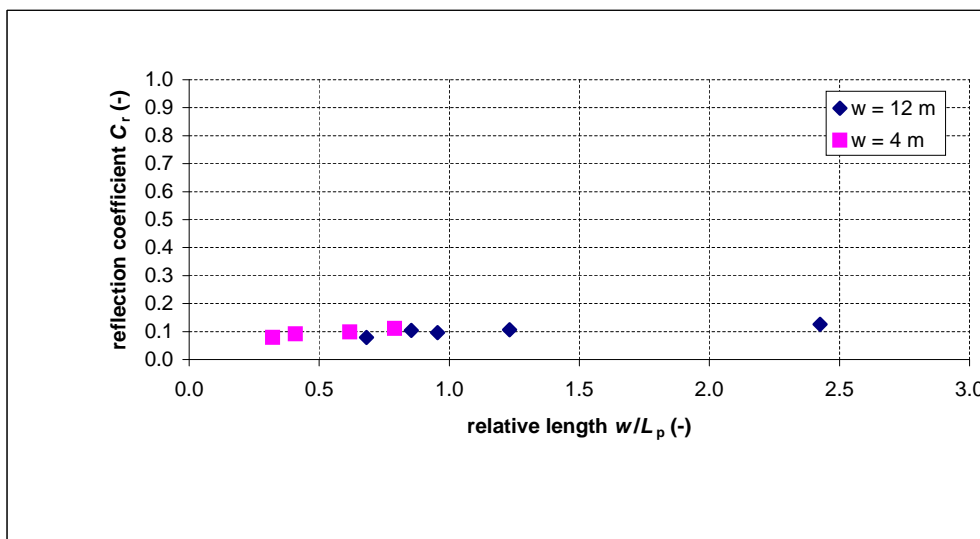
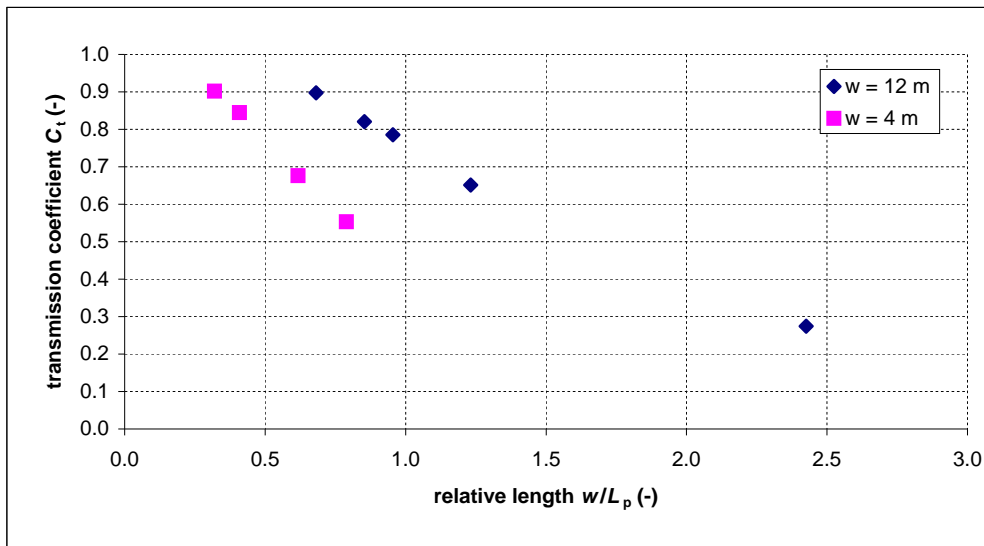
**Deltares**

1200193-005

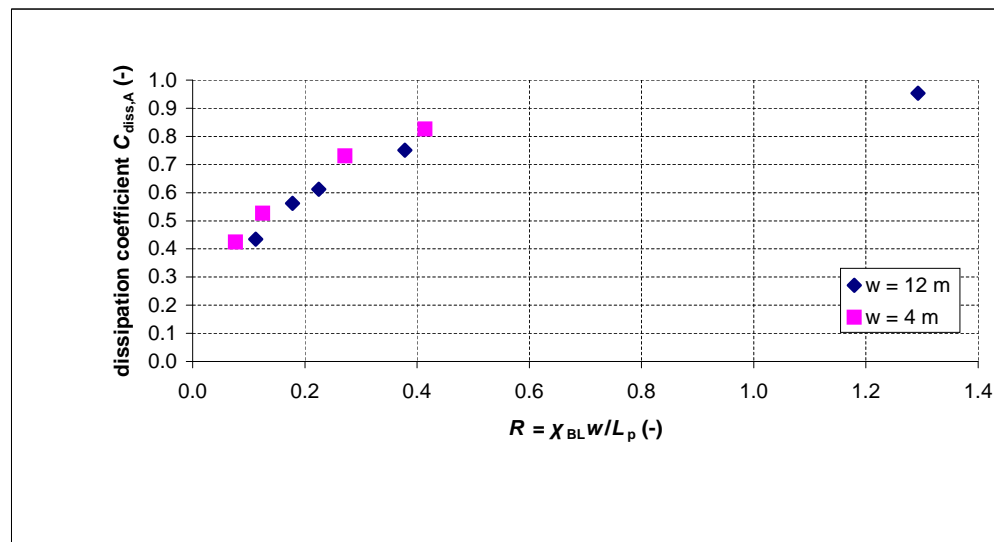
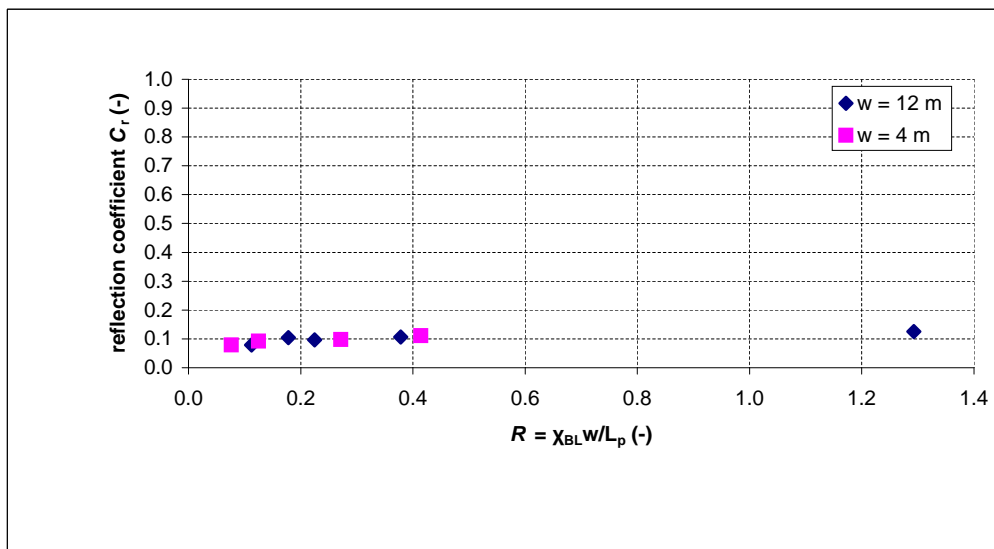
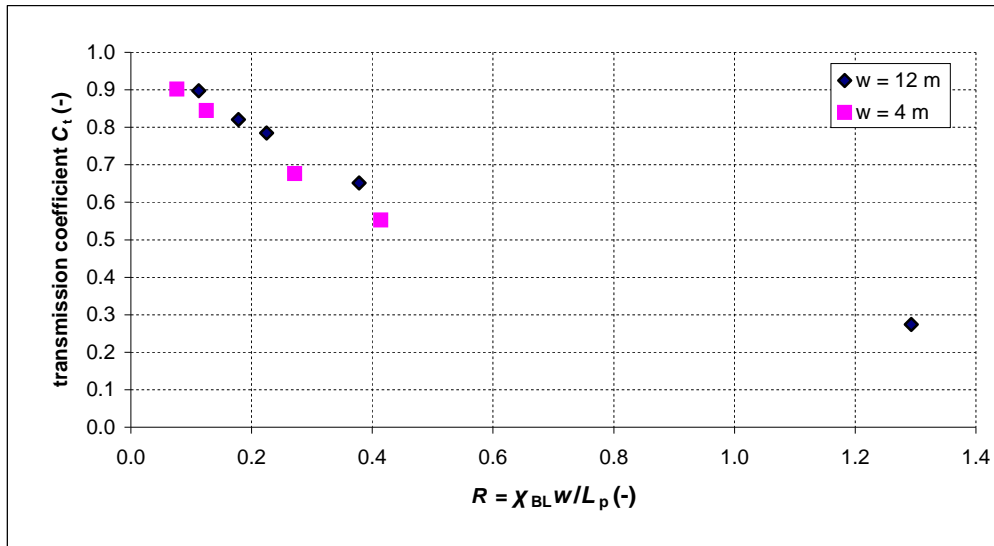
Fig. B.2



Transmission, reflection and dissipation coefficient as function of the significant wave height  $H_{m0}$



Transmission, reflection and dissipation coefficient as function of the relative mattress length  $w/L_p$



Transmission, reflection and dissipation coefficient as function of the relative mattress length and vertical distribution of wave energy  $(w/L_p)\chi$



## **C Photographs**

*Photo C.1 Construction of mattresses (1)*

*Photo C.2 Construction of mattresses (2)*

*Photo C.3 Mattresses after construction*

*Photo C.4 Mattresses during wave experiments*

*Photo C.5 Mattresses during wave experiment (2)*

*Photo C.6 Mattresses with a total length of 4 m*

*Photo C.7 Damage on mattresses after a test (1)*

*Photo C.8 Damage on mattresses after a test (2)*







Construction of mattresses (1)





Construction of mattresses (2)

(Test Series 200)

**Deltares**

1200193-005

Fig. C.2





Mattresses after construction

(Test Series 200)

**Deltares**

1200193-005

Fig. C.3





Mattresses during wave experiments

(Test Series 200)

**Deltares**

1200193-005

Fig. C.4





Mattresses during wave experiment (2)

(Test Series 200)

**Deltares**

1200193-005

Fig. C.5





Matresses with a total length of 4 m

Test Series T300

**Deltares**

1200193-005

Fig. C.6





Damage on mattresses after a test (1)

**Deltares**

1200193-005

Fig. C.7





Damage on mattresses after a test (2)



## **D Exceedance curves and energy density spectra**

*Figure D.1 Exceedance curve and energy density spectra for Test T201*

*Figure D.2 Exceedance curve and energy density spectra for Test T202*

*Figure D.3 Exceedance curve and energy density spectra for Test T204*

*Figure D.4 Exceedance curve and energy density spectra for Test T205*

*Figure D.5 Exceedance curve and energy density spectra for Test T203*

*Figure D.6 Exceedance curve and energy density spectra for Test T301*

*Figure D.7 Exceedance curve and energy density spectra for Test T302*

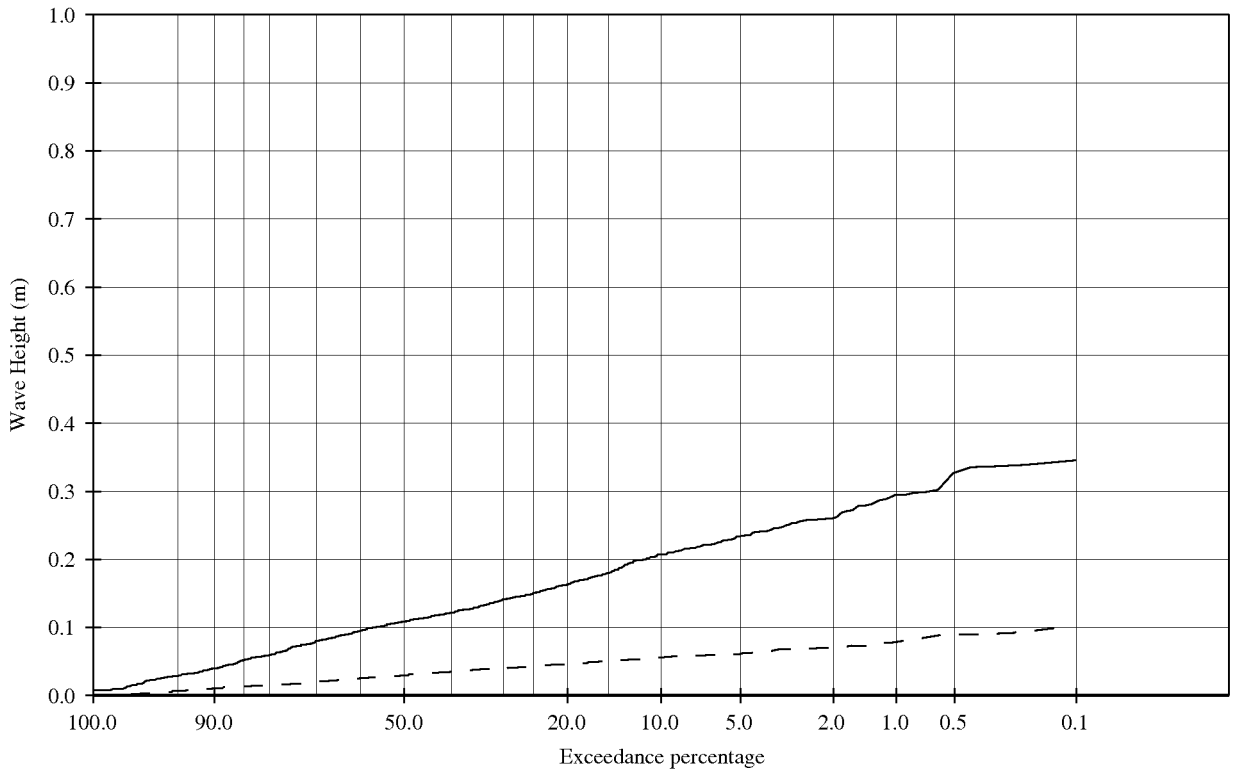
*Figure D.8 Exceedance curve and energy density spectra for Test T305*

*Figure D.9 Exceedance curve and energy density spectra for Test T308*

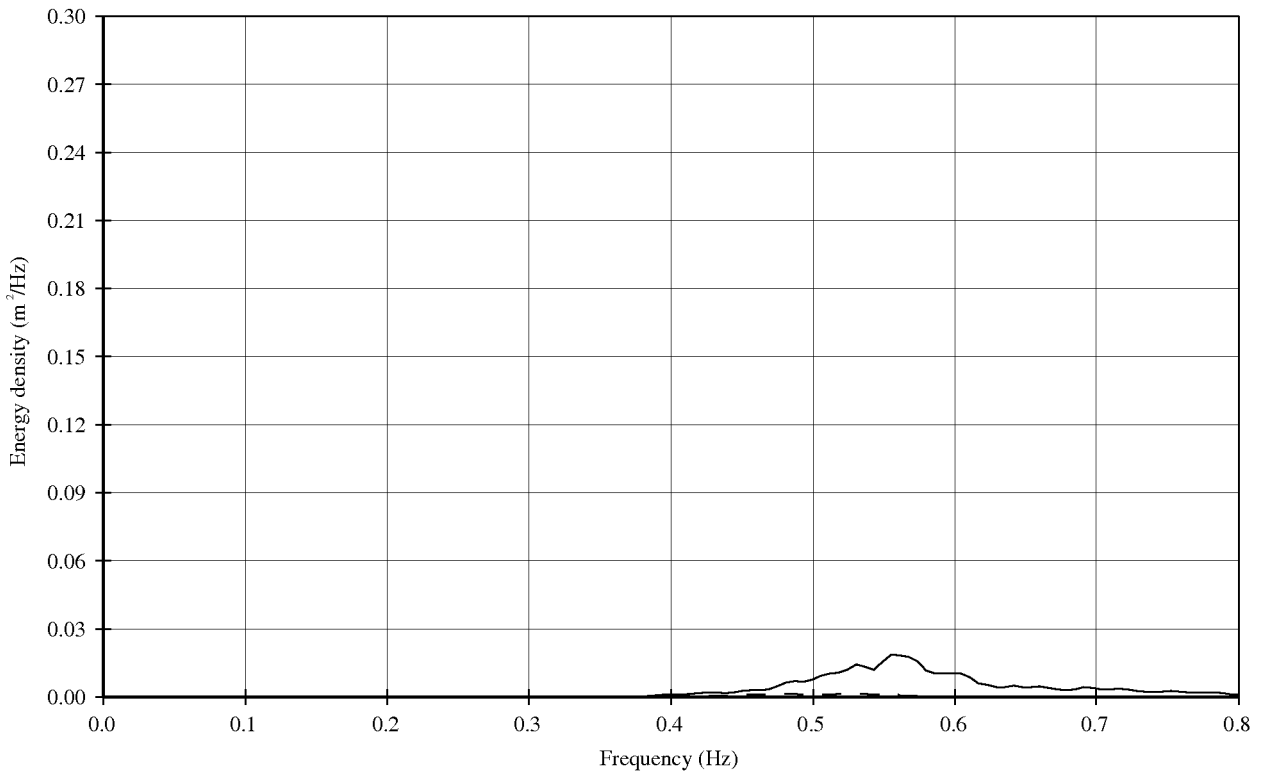
*Figure D.10 Exceedance curve and energy density spectra for Test T601*

*Figure D.11 Exceedance curve and energy density spectra for Test T603*





— Incoming GHM 11;12;13 (Seaside of mattress)  
 - - - Incoming WHM 1;2;3 (Landside of mattress)



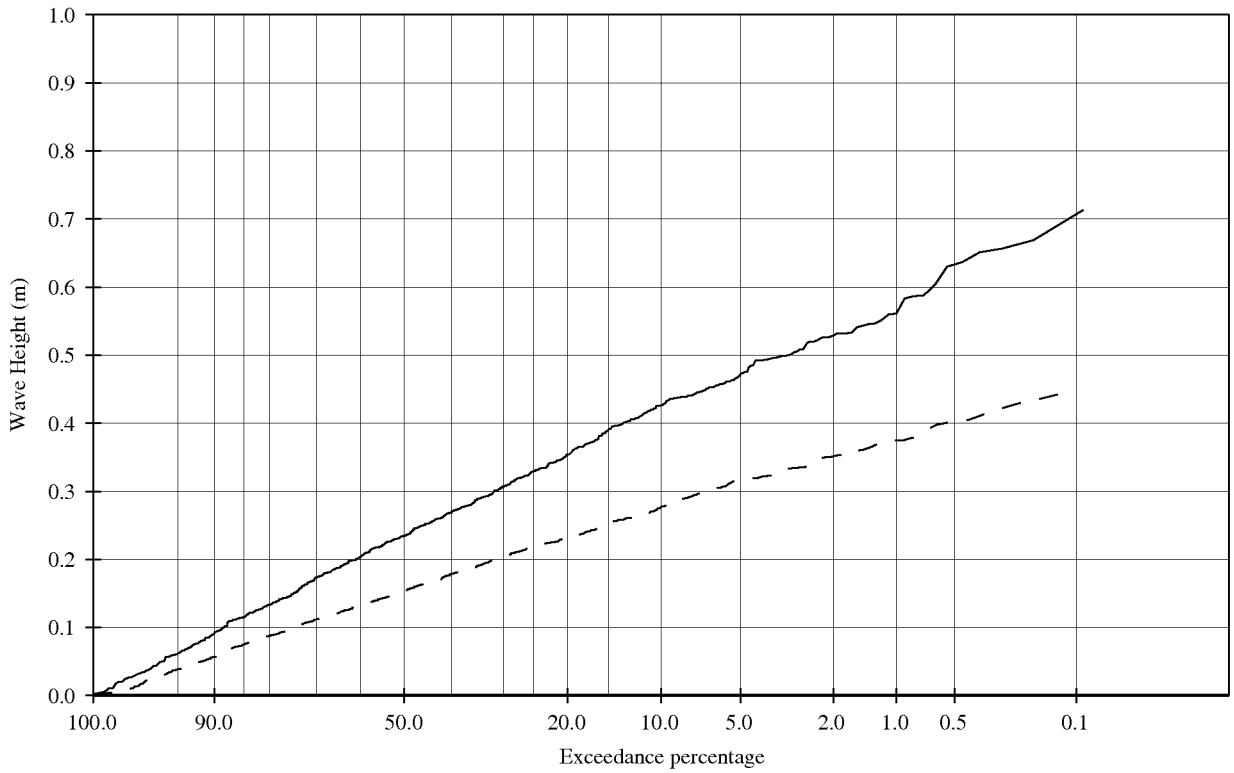
Wave height exceedance curves and  
 energy spectra.

T201

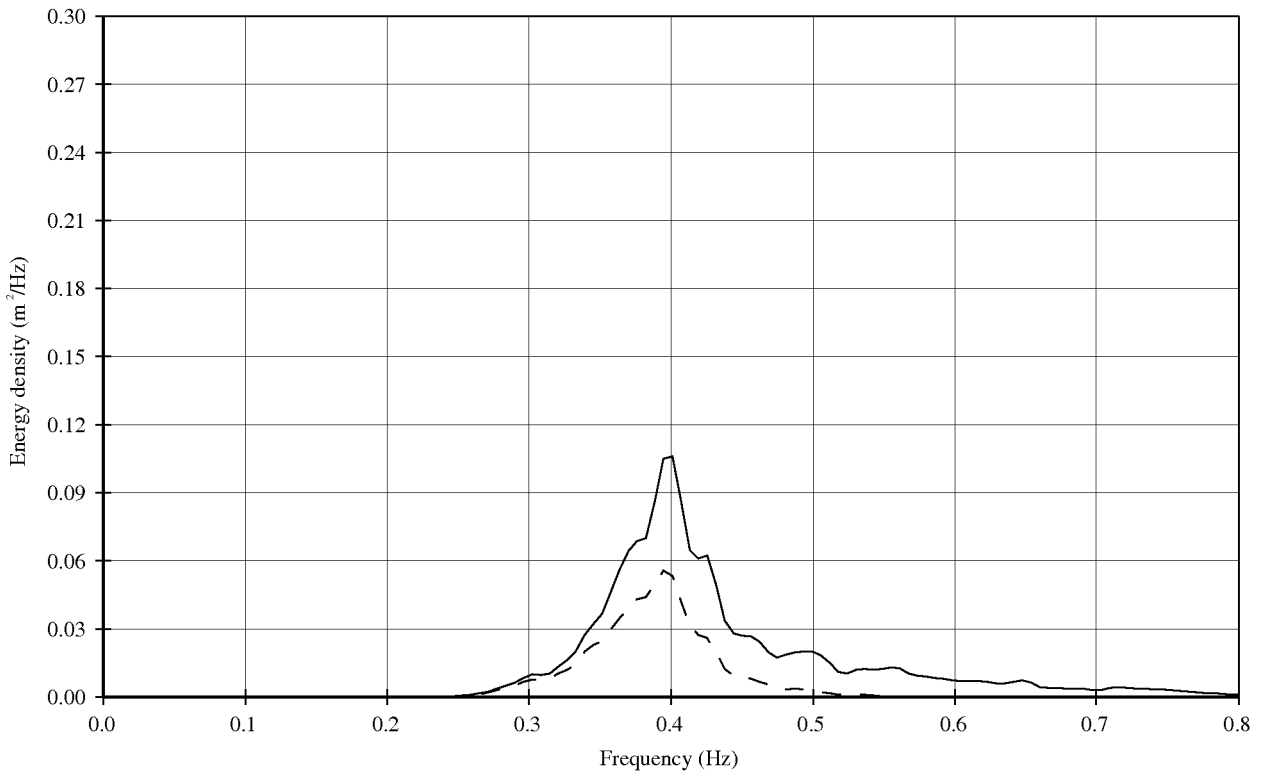
**Deltares**

1202393.005

FIG. D.1



———— Incoming GHM 11;12;13 (Seaside of mattress)  
 - - - - Incoming WHM 1;2;3 (Landside of mattress)



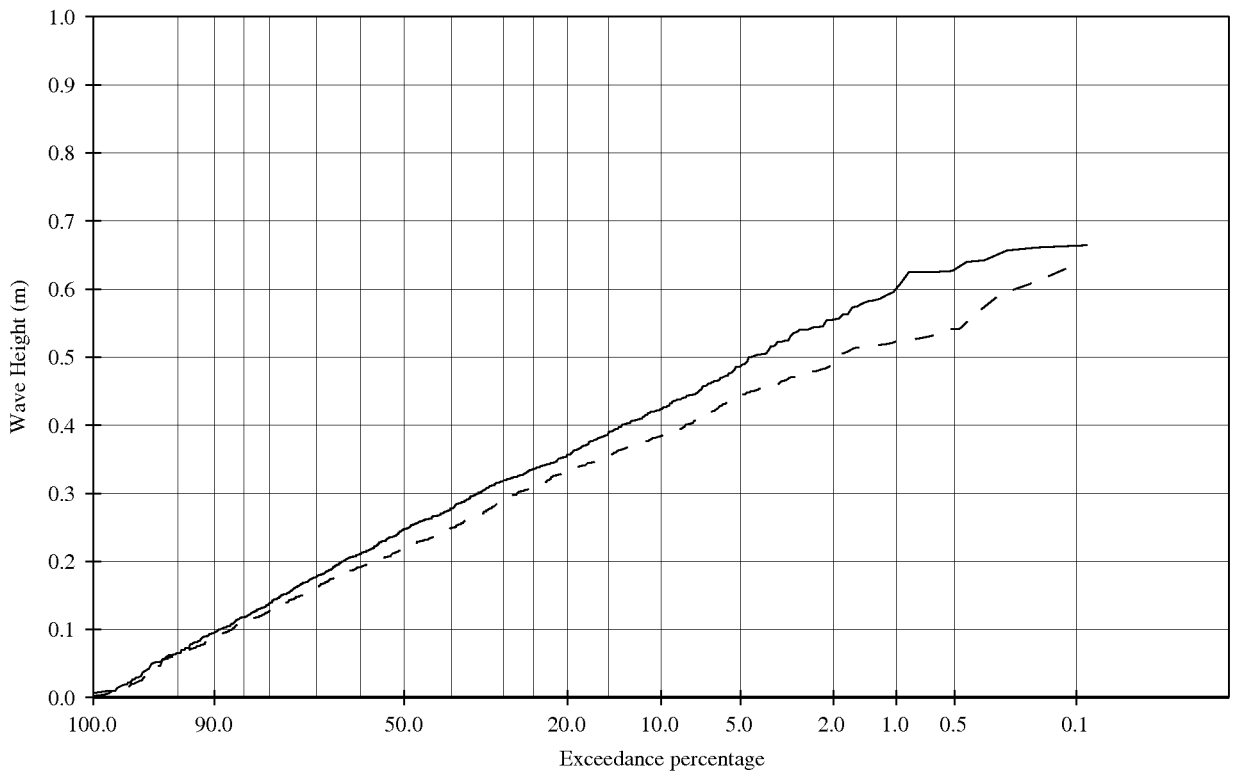
Wave height exceedance curves and  
 energy spectra.

T202

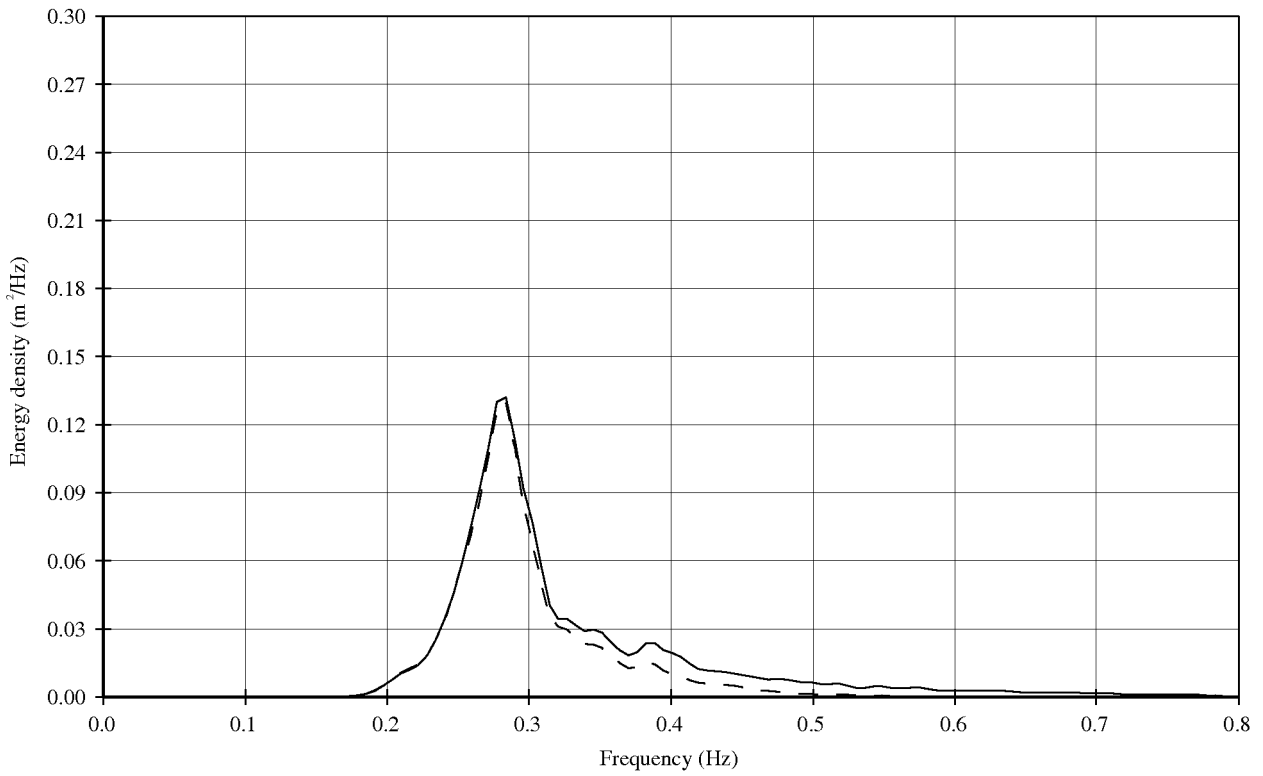
**Deltares**

1202393.005

FIG. D.2



———— Incoming GHM 11;12;13 (Seaside of mattress)  
 - - - - Incoming WHM 1;2;3 (Landside of mattress)



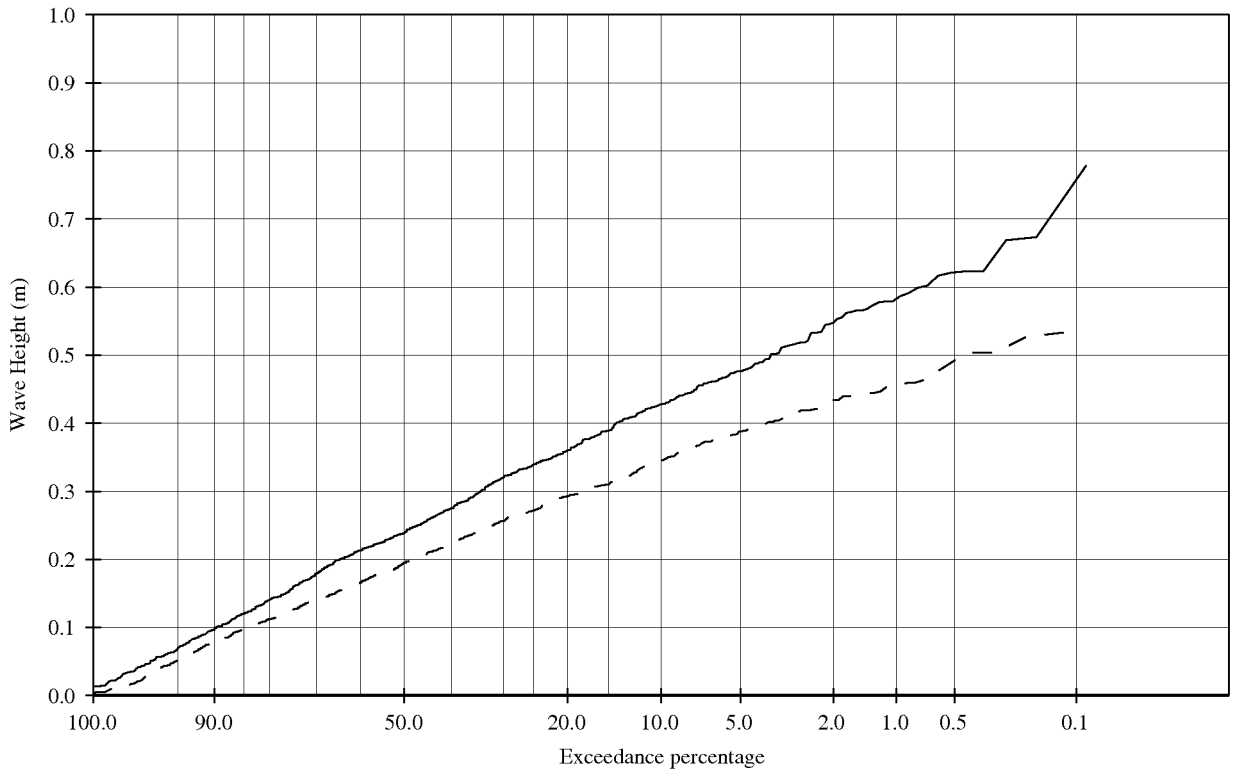
Wave height exceedance curves and  
 energy spectra.

T204

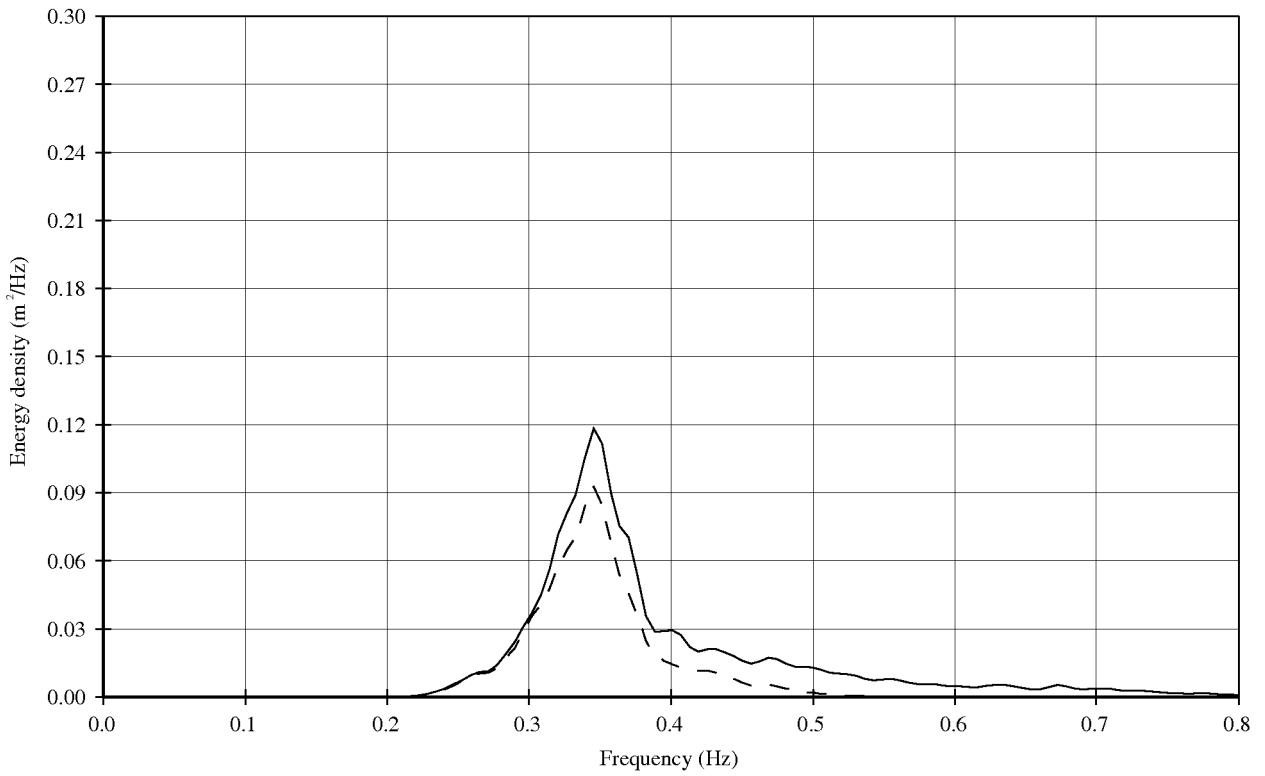
**Deltares**

1202393.005

FIG. D.3



———— Incoming GHM 11;12;13 (Seaside of mattress)  
 - - - - Incoming WHM 1;2;3 (Landside of mattress)



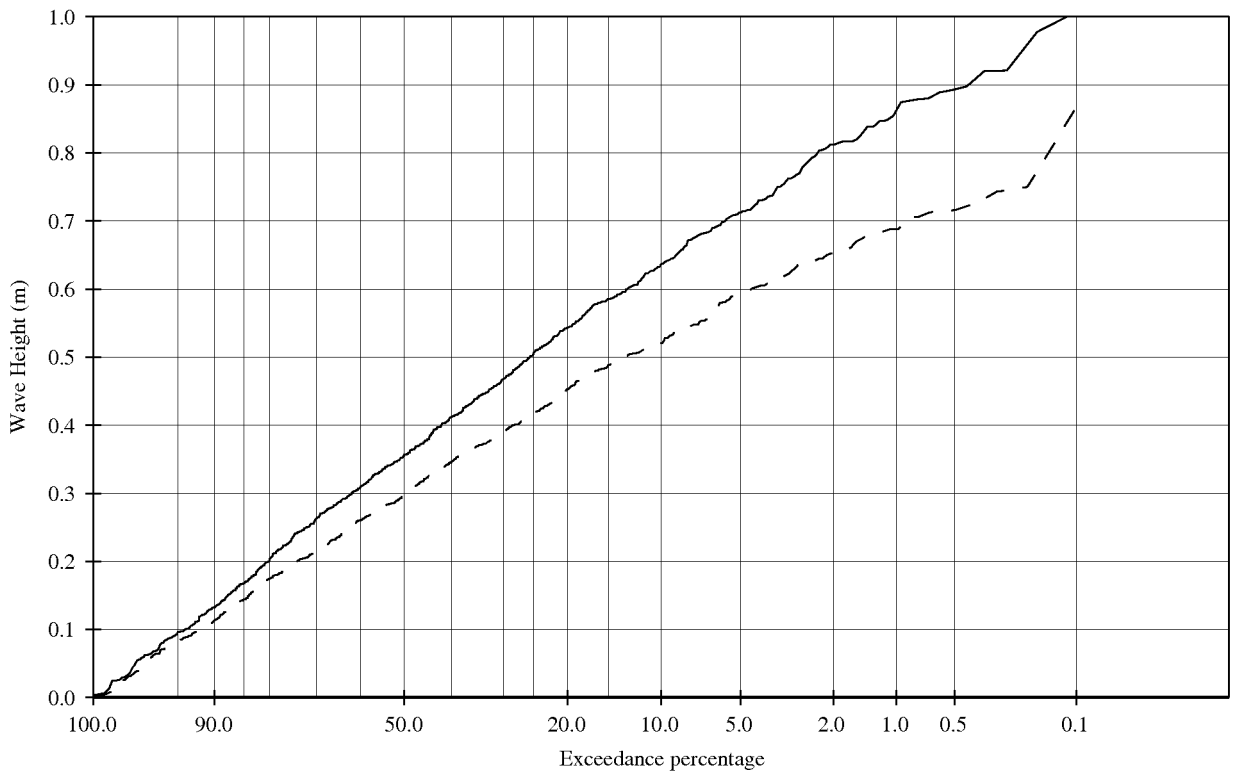
Wave height exceedance curves and  
 energy spectra.

T205

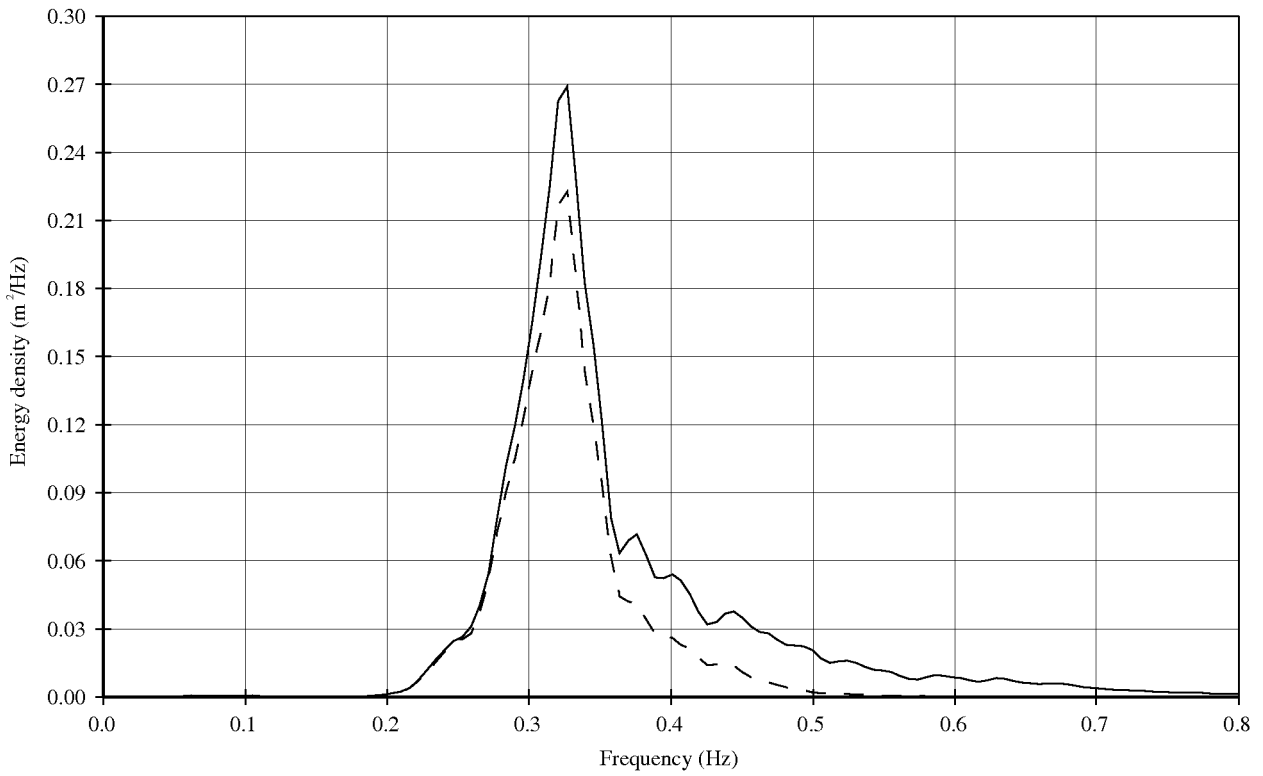
**Deltares**

1202393.005

FIG. D.4



— Incoming GHM 11;12;13 (Seaside of mattress)  
 - - - Incoming WHM 1;2;3 (Landside of mattress)



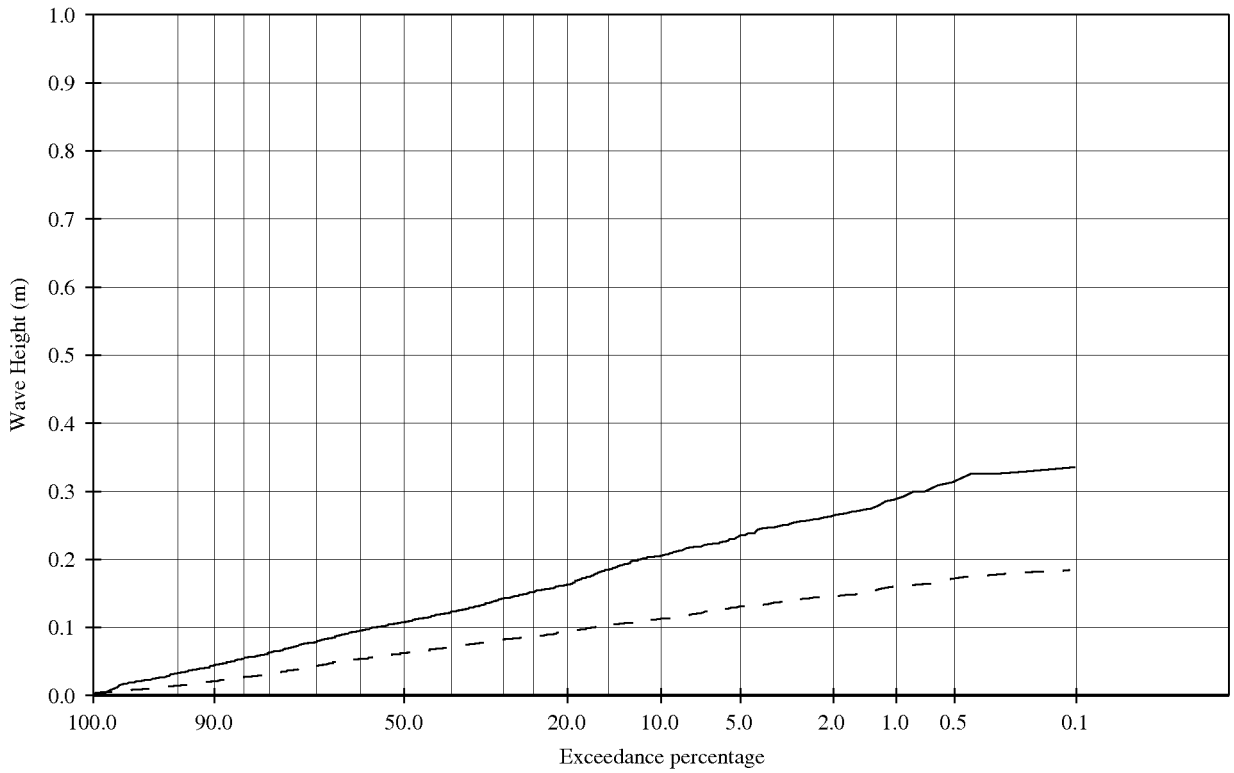
Wave height exceedance curves and  
 energy spectra.

T203

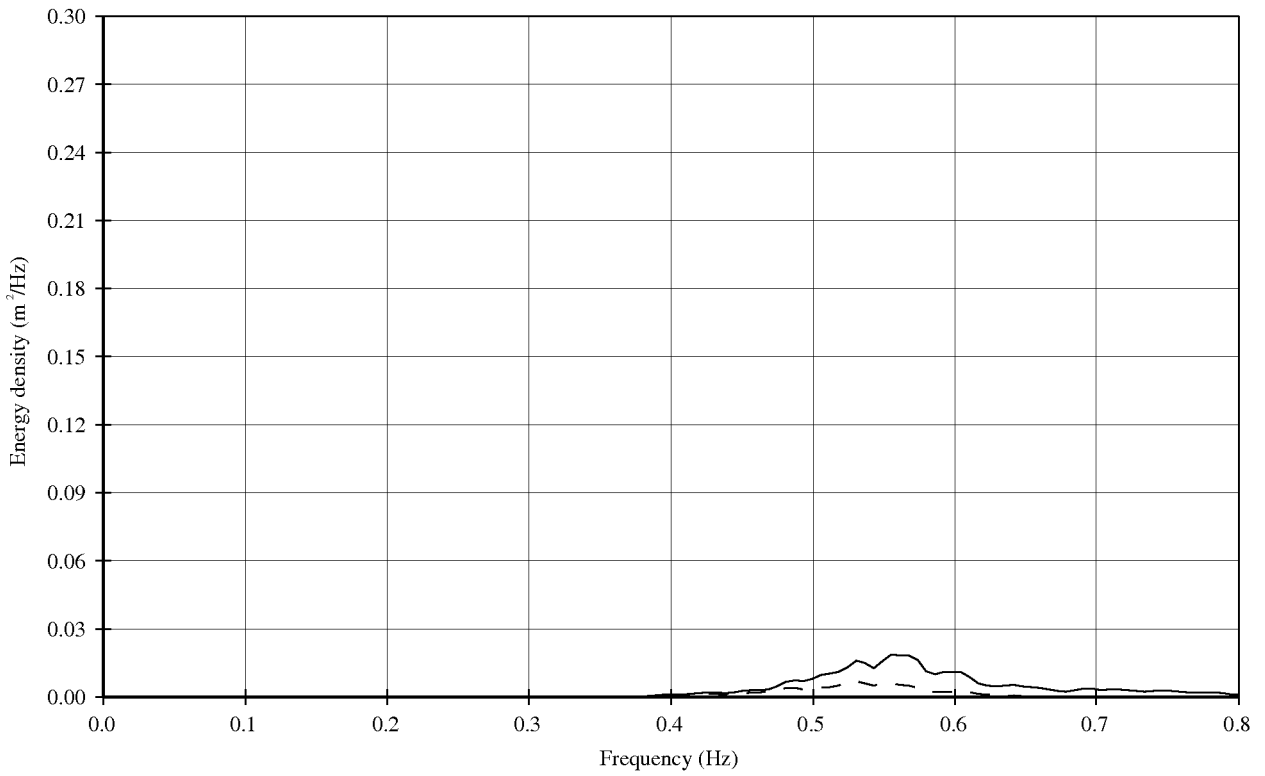
**Deltares**

1202393.005

FIG. D.5



— Incoming GHM 11;12;13 (Seaside of mattress)  
 - - - Incoming WHM 1;2;3 (Landside of mattress)



Wave height exceedance curves and  
 energy spectra.

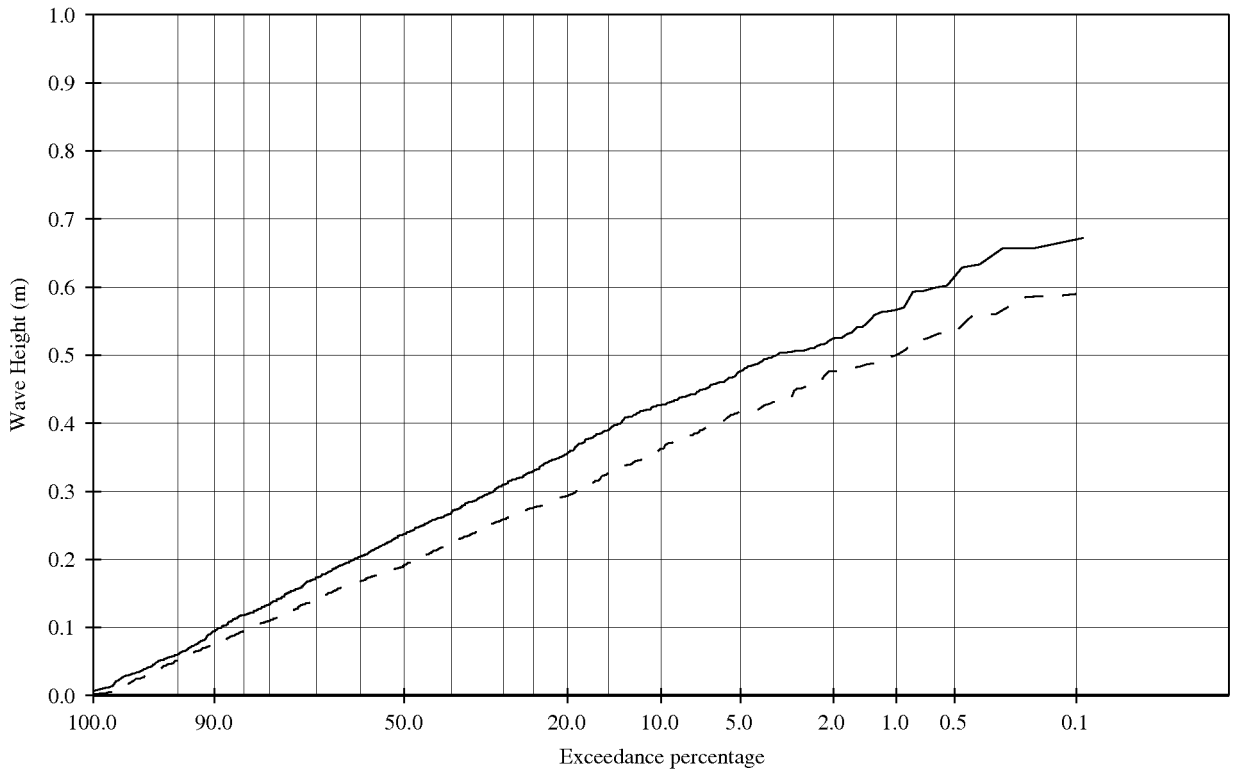
T301

Deltares

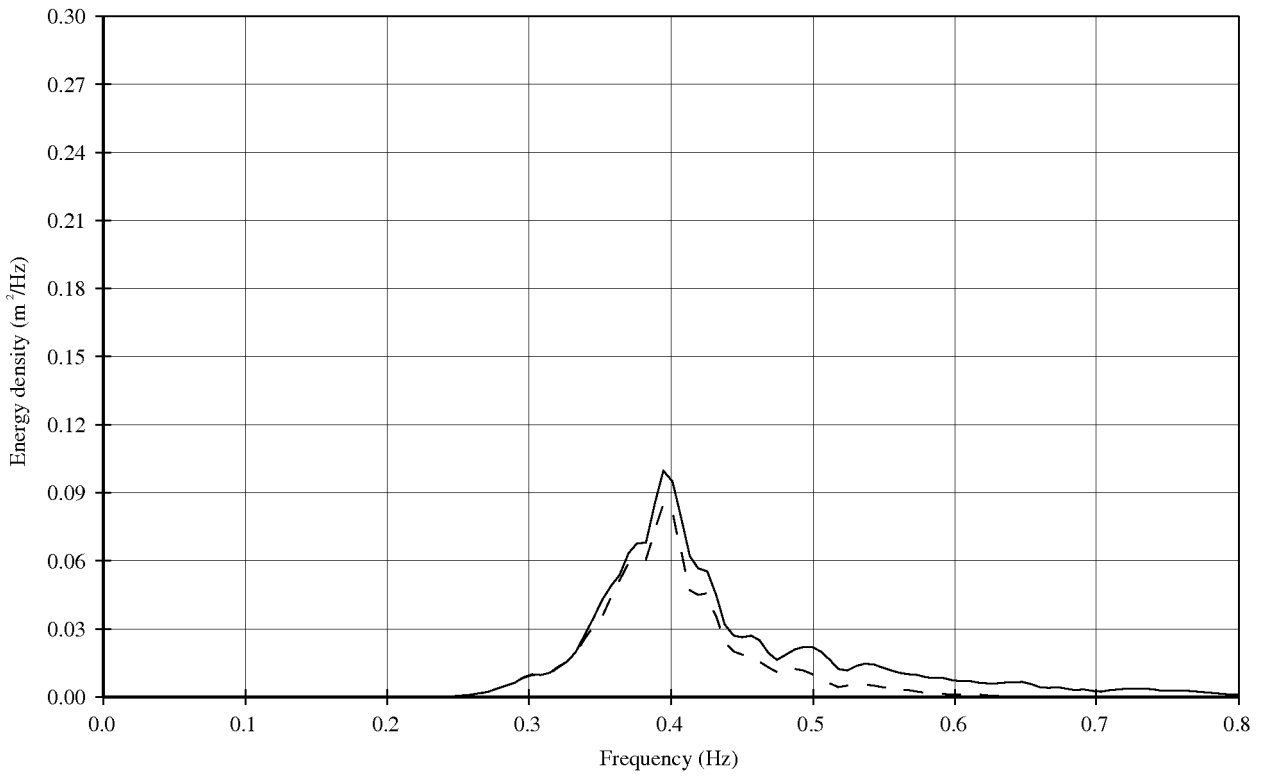
1202393.005

FIG. D.6





———— Incoming GHM 11;12;13 (Seaside of mattress)  
 - - - - Incoming WHM 1;2;3 (Landside of mattress)



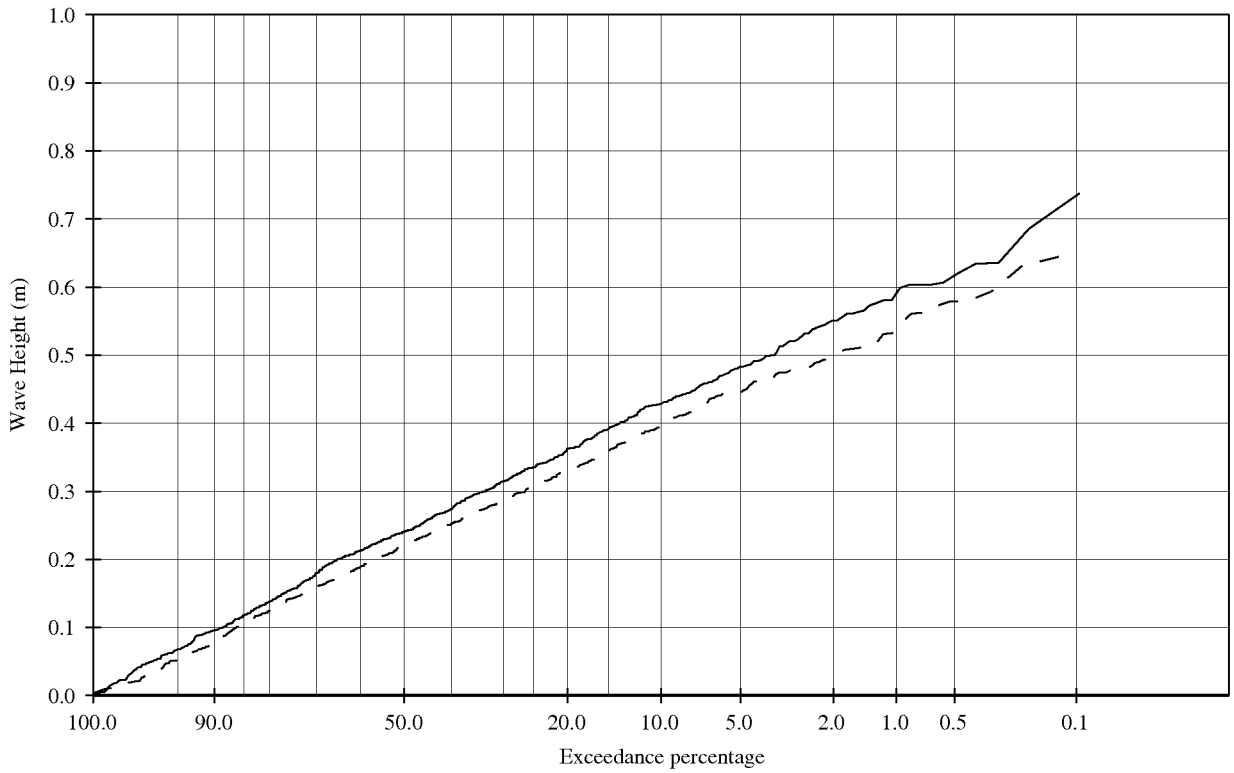
Wave height exceedance curves and  
 energy spectra.

T302

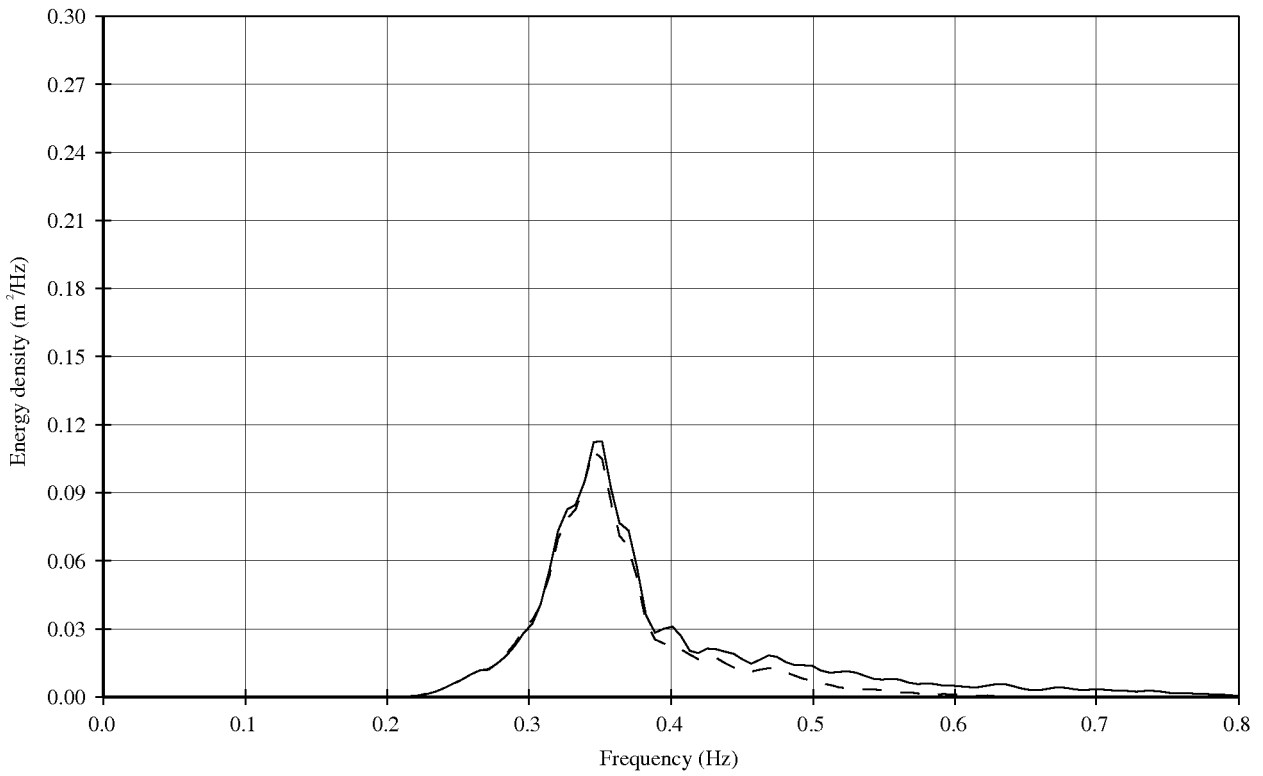
**Deltares**

1202393.005

FIG. D.7



———— Incoming GHM 11;12;13 (Seaside of mattress)  
 - - - - Incoming WHM 1;2;3 (Landside of mattress)



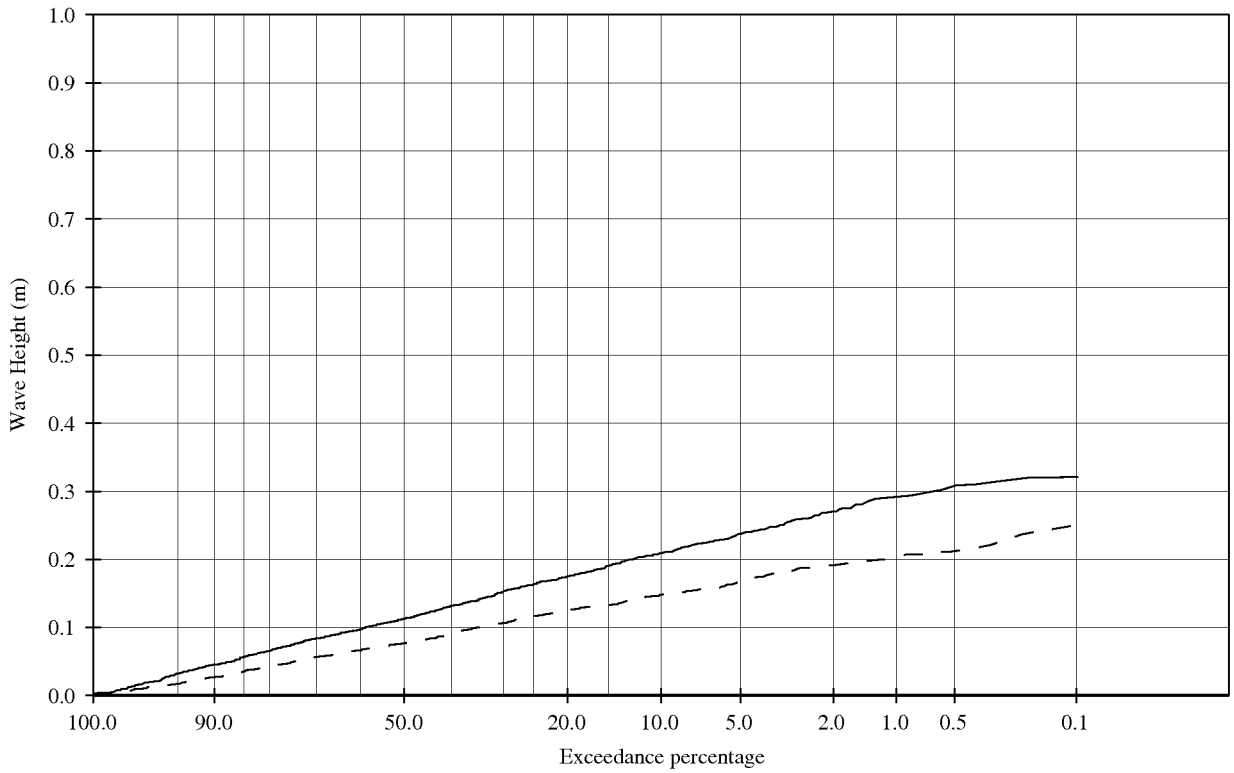
Wave height exceedance curves and  
 energy spectra.

T305

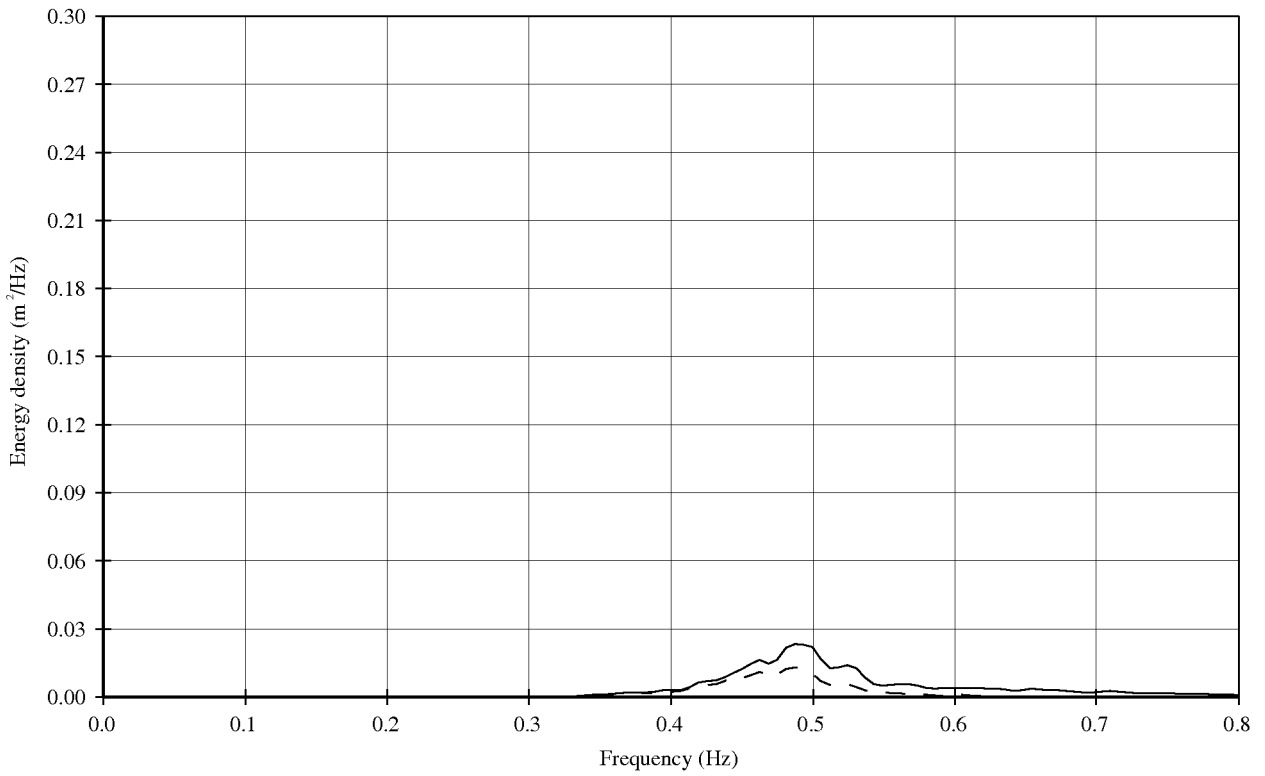
Deltares

1202393.005

FIG. D.8



———— Incoming GHM 11;12;13 (Seaside of mattress)  
 - - - - - Incoming WHM 1;2;3 (Landside of mattress)



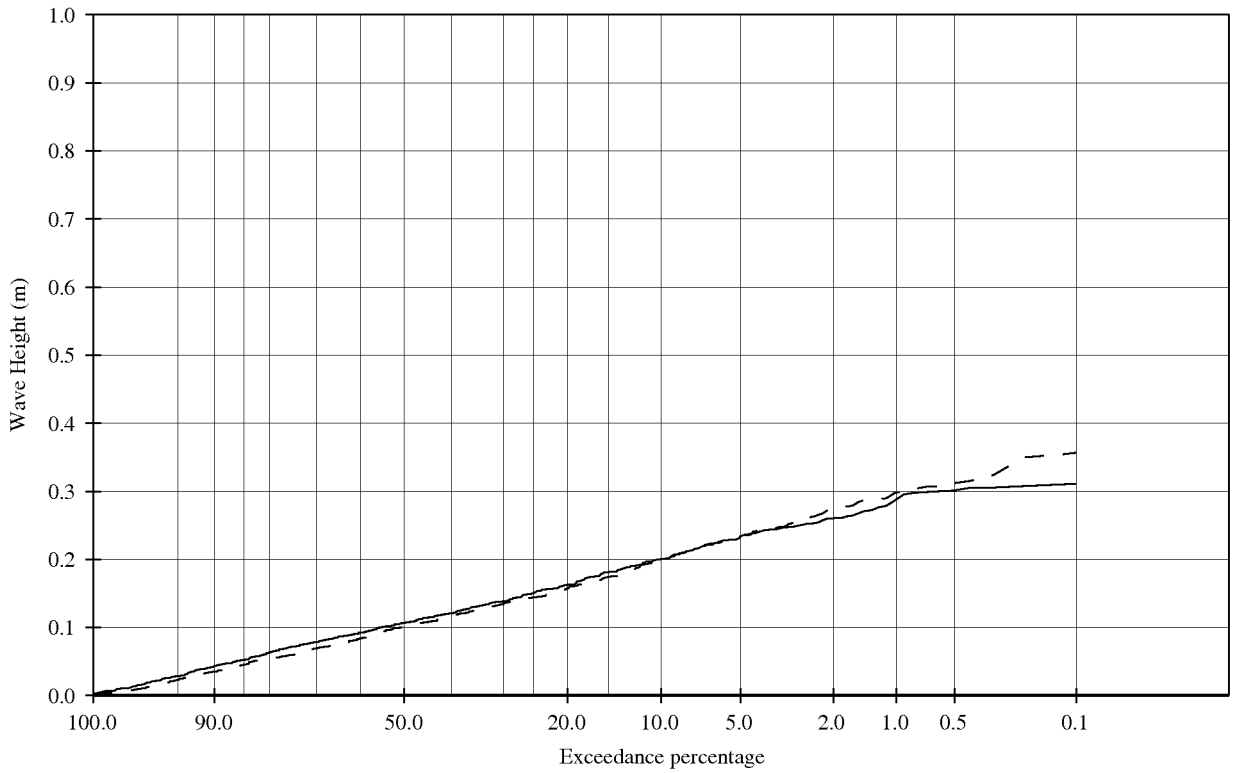
Wave height exceedance curves and  
 energy spectra.

T308

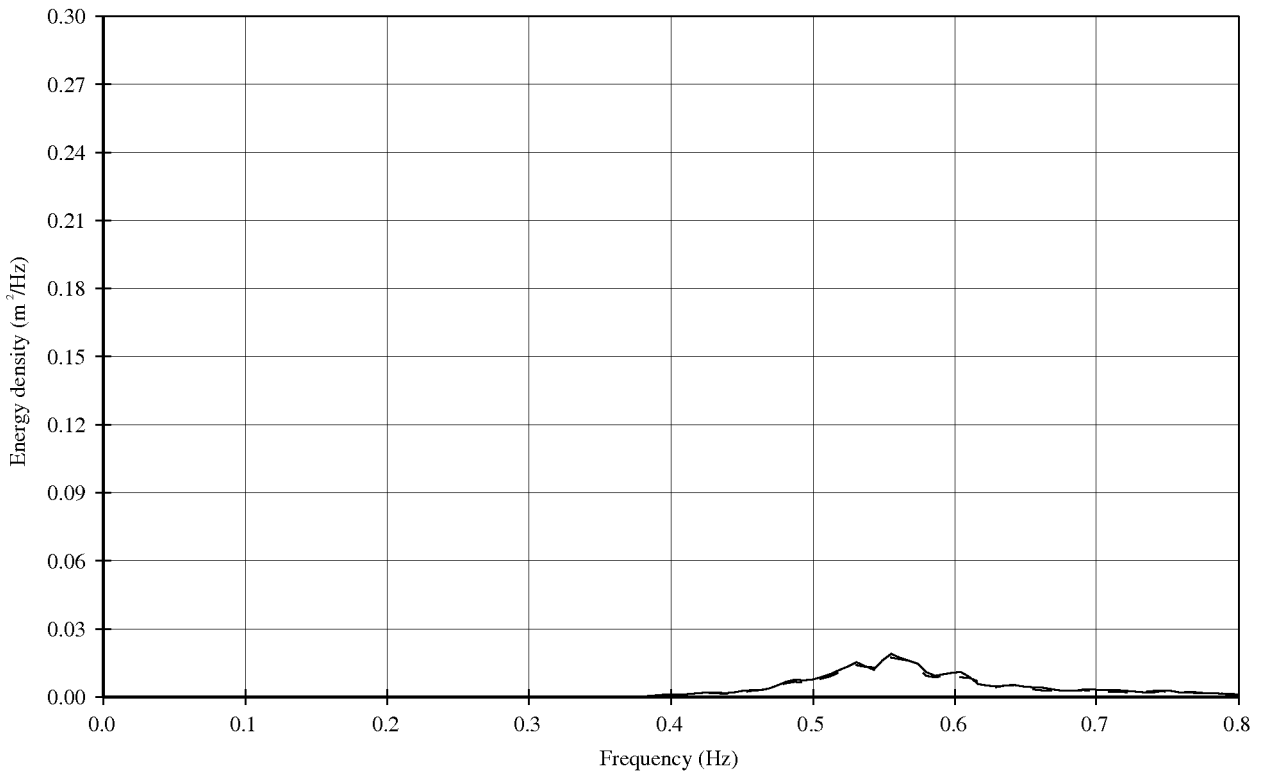
**Deltares**

1202393.005

FIG. D.9



———— Incoming GHM 11;12;13 (Seaside of mattress)  
 - - - - Incoming WHM 1;2;3 (Landside of mattress)



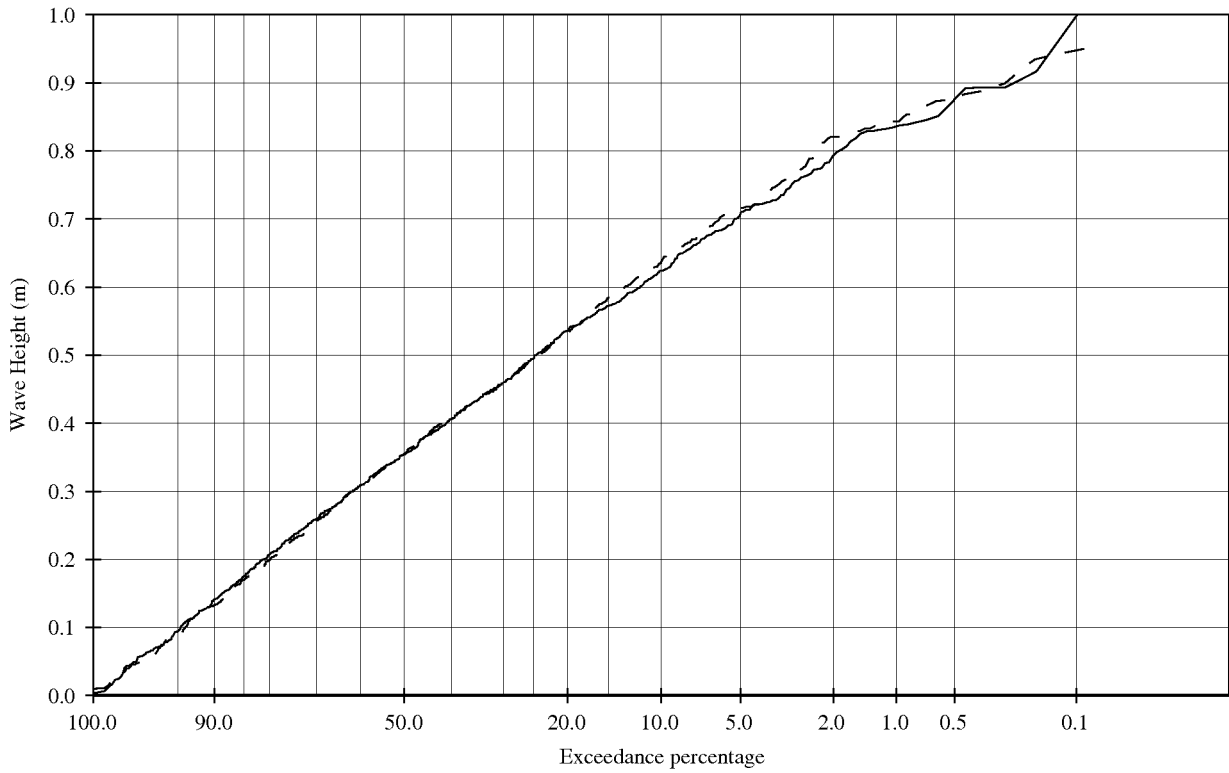
Wave height exceedance curves and  
 energy spectra.

T601

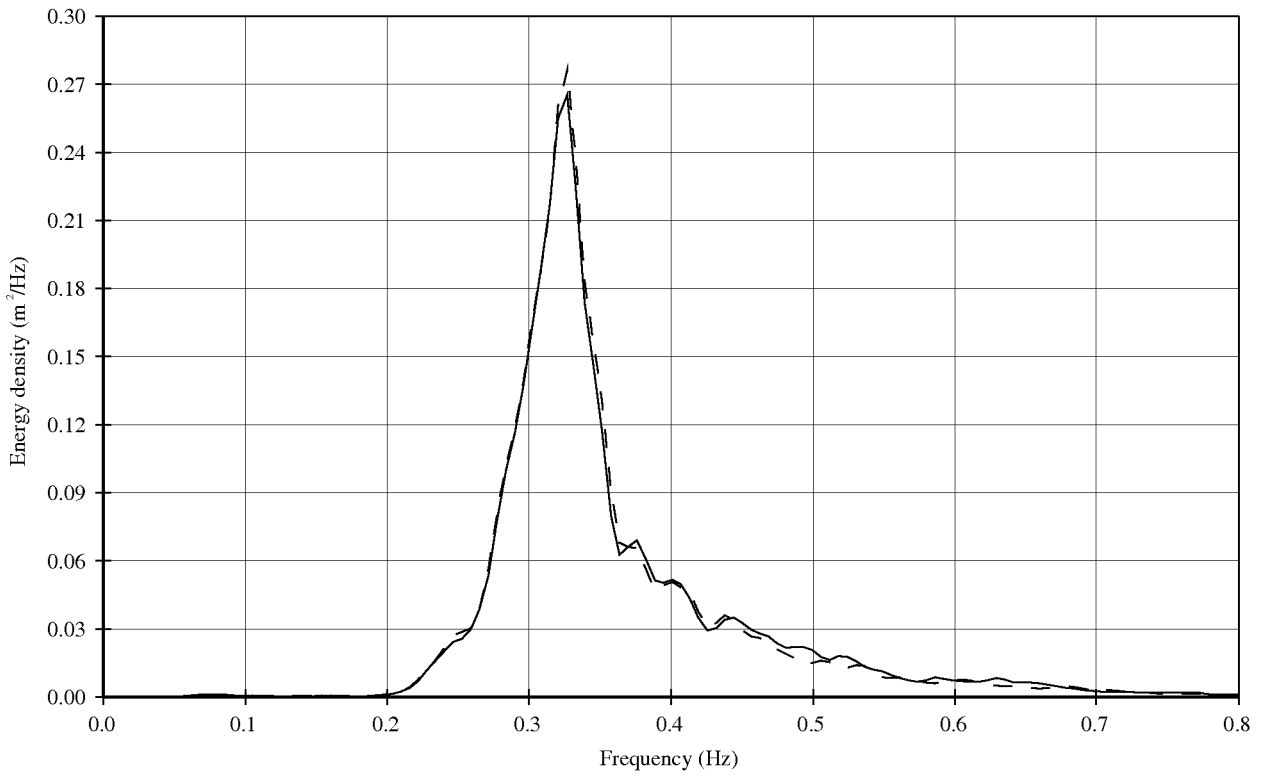
**Deltares**

1202393.005

FIG. D.10



———— Incoming GHM 11;12;13 (Seaside of mattress)  
 - - - - Incoming WHM 1;2;3 (Landside of mattress)



Wave height exceedance curves and  
 energy spectra.

T603

**Deltares**

1202393.005

FIG. D.11



## E Theoretical background: determination of reflected, transmitted and dissipated wave energy

This section describes an approach to determine the ratio between the reflected energy ( $E_r$ ) and the dissipated energy ( $E_{diss}$ ).

It is assumed that wave measurements with three wave gauges are performed before and after the floating structure. By using three wave gauges, the incident and reflected wave (energy) can be measured using the technique as described in Mansard and Funke (1980). Wave measurements were performed at two locations: one location in front of the structure (Location 1) and one location behind the structure (Location 2). In total four parameters were measured: incident wave energy at Location 1 ( $E_{i,WHM1}$ ) and Location 2 ( $E_{i,WHM2}$ ) and the reflected wave energy at Location 1 ( $E_{r,WHM1}$ ) and Location 2 ( $E_{r,WHM2}$ ).

When the wave approaches the floating structure, the energy is partly reflected ( $E_r$ ) partly dissipated ( $E_{diss}$ ) and partly transmitted ( $E_t$ ). This is illustrated in Figure E.1. How the wave measurements ( $E_{i,WHM1}$ ,  $E_{i,WHM2}$ ,  $E_{r,WHM1}$  and  $E_{r,WHM2}$ ) leads to individual values for reflected wave energy ( $E_{r,A}$ ,  $E_{r,B}$ ), transmitted wave energy ( $E_{t,A}$ ,  $E_{t,B}$ ) and dissipated wave energy ( $E_{diss,A}$ ,  $E_{diss,B}$ ) is explained below.

The relation between energy and wave heights is the following:

$$C_t = \sqrt{\frac{E_t}{E_i}} = \frac{H_t}{H_i} \quad (4.1)$$

$$C_r = \sqrt{\frac{E_r}{E_i}} = \frac{H_r}{H_i} \quad (4.2)$$

$$C_{diss} = \sqrt{\frac{E_{diss}}{E_i}} \quad (4.3)$$

It is assumed that the waves are fully absorbed by the wave paddle. Besides this, it is assumed that the waves that reflect from the damping slope are not re-reflected at the floating structure ( $E_{r,C} = 0$ ).

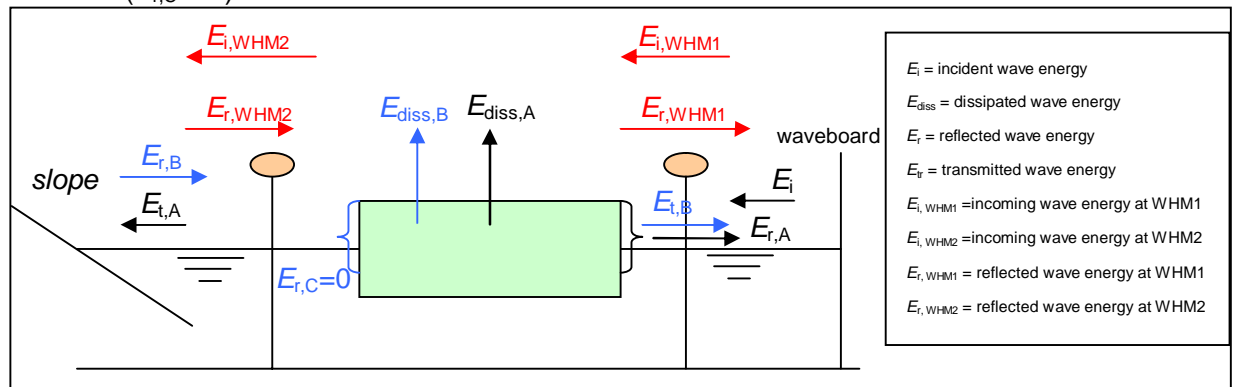


Figure E.1 Schematisation of the model set-up for an irregular wave field

Based on Figure E.1, the following equations are derived:

$$E_i = E_{i,WHM1} \quad (4.4)$$

$$E_{t,A} + E_{r,C} = E_{i,WHM2} \quad (4.5)$$

$$E_{r,A} + E_{t,B} = E_{r,WHM1} \quad (4.6)$$

$$E_i = E_{r,A} + E_{diss,A} + E_{t,A} \quad (4.7)$$

$$E_{r,B} = E_{r,WHM2} \quad (4.8)$$

$$E_{r,B} = E_{r,C} + E_{diss,B} + E_{t,B} \quad (4.9)$$

$$E_{r,C} = 0 \text{ (assumption)} \quad (4.10)$$

Unfortunately, it is not possible to solve these equations. An additional equation is required based on the assumption that the transmission coefficient  $C_t$  is in both directions the same:

$$C_{t,A} = C_{t,B} \quad (4.11)$$

$$C_{t,A} = \sqrt{\frac{E_{t,A}}{E_i}} \quad (4.12)$$

$$C_{t,B} = \sqrt{\frac{E_{t,B}}{E_{r,B}}} \quad (4.13)$$

Combining Equation (4.11) until Equation (4.13) gives:

$$E_{t,A} E_{r,B} = E_{t,B} \cdot E_i \quad (4.14)$$

Now it is possible to solve the equations:

$$\text{(based on Eq. (4.14))}: E_{t,B} = \frac{E_{t,A} E_{r,B}}{E_i} = \frac{E_{i,WHM2} E_{r,WHM2}}{E_{i,WHM1}} \quad (4.15)$$

$$\text{(based on Eq. (4.9))}: E_{diss,B} = E_{r,B} - E_{r,C} - E_{t,B} = E_{r,WHM2} - \frac{E_{i,WHM2} E_{r,WHM2}}{E_{i,WHM1}} \quad (4.16)$$

$$\text{(based on Eq.(4.6))}: E_{r,A} = E_{r,WHM1} - E_{t,B} = E_{r,WHM1} - \frac{E_{i,WHM2} E_{r,WHM2}}{E_{i,WHM1}} \quad (4.17)$$

(based on Eq.(4.7)):

$$E_{diss,A} = E_i - E_{r,A} - E_{t,A} = E_{i,WHM1} - E_{r,WHM1} + \frac{E_{i,WHM2} E_{r,WHM2}}{E_{i,WHM1}} - E_{i,WHM2} \quad (4.18)$$



$$\alpha = \frac{E_{diss,A}}{E_{r,A}} \tag{4.19}$$

All relevant parameters are now expressed as a function of measurable parameters. An overview of the resulting formulae is given in Table E.1.

*Table E.1 Overview determination incident, transmitted and reflected wave energy for an irregular wave field*

$E_i = E_{i,WHM1}$
$E_{t,A} = E_{i,WHM2}$
$E_{t,B} = \frac{E_{i,WHM2} E_{rWHM2}}{E_{i,WHM1}}$
$E_{r,A} = E_{r,WHM1} - \frac{E_{i,WHM2} E_{rWHM2}}{E_{i,WHM1}}$
$E_{r,B} = E_{r,WHM2}$
$E_{r,C} = 0$
$E_{diss,A} = E_{i,WHM1} - E_{r,WHM1} + \frac{E_{i,WHM2} E_{rWHM2}}{E_{i,WHM1}} - E_{i,WHM2}$
$E_{diss,B} = E_{r,WHM2} - \frac{E_{i,WHM2} E_{rWHM2}}{E_{i,WHM1}}$
$\alpha = \frac{E_{diss,A}}{E_{r,A}}$



## F Theoretical derivation of $\chi$

Ratio of non-blocked energy  $\chi_{TR}$  is defined by:

$$\chi_{tr} = \frac{E_{transmitted}}{E_{incident}} = 1 - \frac{E_{blocked}}{E_{incident}} \quad (5.1)$$

Kinetic energy is assumed to be proportional with maximum horizontal velocity in orbital motion:

$$E \propto u_{hor,max}^2 \quad (5.2)$$

With, according to linear wave theory

$$u_{hor,max} = \omega a \frac{\cosh k(h+z)}{\sinh kh} \quad \text{or} \quad u_{hor,max}^2 \propto \cosh^2 k(h+z) \quad (5.3)$$

Eq. (5.3) is rewritten as

$$E(z) \propto u_{hor,max}^2 \propto \cosh 2k(h+z) + 1 \quad (5.4)$$

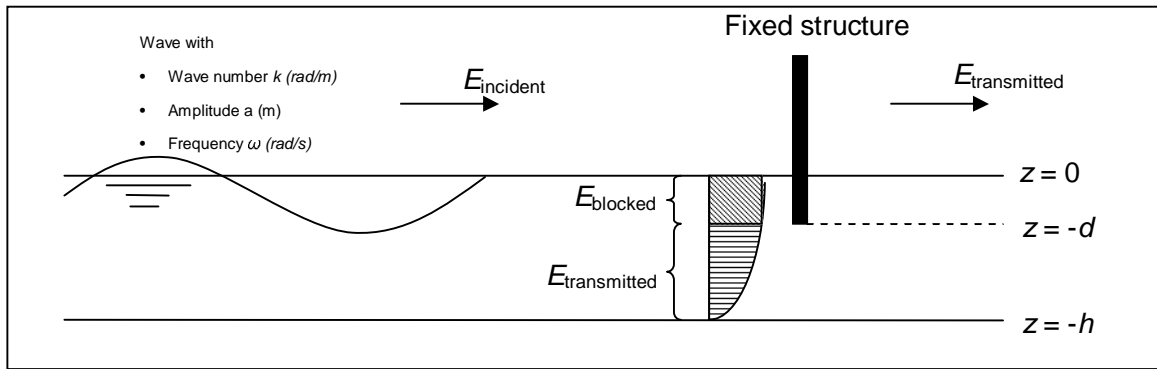


Figure F.1 Schematisation of fixed structure blocking wave energy

Combining Eq. (5.1) and Eq. (5.4) gives:

$$\chi_{tr} = 1 - \frac{\int_{-d}^0 Edz}{\int_{-h}^0 Edz} = 1 - \frac{\int_{-d}^0 (\cosh 2k(h+z) + 1) dz}{\int_{-h}^0 (\cosh 2k(h+z) + 1) dz} = 1 - \frac{\left[ \frac{1}{2k} \sinh 2k(h+z) + z \right]_{-d}^0}{\left[ \frac{1}{2k} \sinh 2k(h+z) + z \right]_{-h}^0} \quad (5.5)$$

or

$$\chi_{tr} = 1 - \frac{\left[ \frac{1}{2k} \sinh 2k(h+0) + 0 \right] - \left[ \frac{1}{2k} \sinh 2k(h-d) - d \right]}{\left[ \frac{1}{2k} \sinh 2k(h+0) + 0 \right] - \left[ \frac{1}{2k} \sinh 2k(h-h) - h \right]} \quad (5.6)$$

or

$$\chi_{tr} = 1 - \frac{\sinh 2kh - \sinh 2k(h-d) + 2kd}{\sinh 2kh + 2kh} \quad (5.7)$$

or

$$\chi_{tr} = \frac{\sinh 2k(h-d) - 2kd + 2kh}{\sinh 2kh + 2kh} \quad (5.8)$$

Eq. (5.8) is also found with Eq. (5.9) as starting point:

$$\chi_{tr} = \frac{\int_0^{-d} Edz}{\int_{-h}^{-d} Edz} \quad (5.9)$$

The ratio of blocked energy is determined by:

$$\chi_{bl} = 1 - \chi_{tr} \quad (5.10)$$

With Eq. (5.6), the energy transmission ratio parameter  $\chi_{tr}$  is written as a function of wave number  $k$ , depth  $h$  and structure depth  $d$ :

$$\chi_{tr} = f(k, d, h) \quad (5.11)$$

Energy component	Ratio
Blocked energy by structure	$\chi_{bl} = \frac{\sinh 2kh - \sinh 2k(h-d) + 2kd}{\sinh 2kh + 2kh}$
Transmitted energy	$\chi_{tr} = \frac{\sinh 2k(h-d) - 2kd + 2kh}{\sinh 2kh + 2kh}$

With

$$\text{wave number} \quad k \text{ (rad/m)} \quad k = \frac{2\pi}{L} \quad (5.12)$$

$$\text{wave length} \quad L \text{ (m)} \quad L = L_o \tanh\left(\frac{2\pi h}{L}\right) \quad (5.13)$$

$$\text{deep water wave length} \quad L_o \text{ (m)} \quad L_o = \frac{gT^2}{2\pi} \quad (5.14)$$

$$\text{water depth} \quad h \text{ (m)}$$

$$\text{structure depth} \quad d \text{ (m)}$$

## G Theoretical determination of dissipation coefficient $C_{\text{diss}}$

To include length effect of a porous structure into the dissipation coefficient  $C_{\text{diss}}$  a porous medium with a length  $w$  is assumed to have  $n$  segments with length  $\Delta x$  as illustrated in Figure G.1.

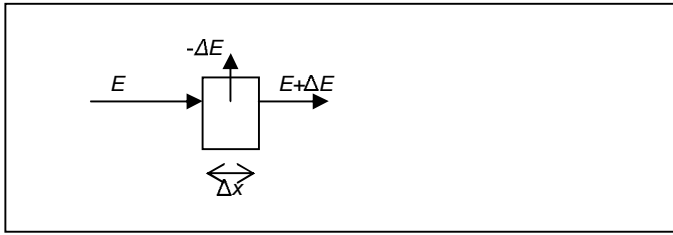


Figure G.1 Dissipation of energy on a porous segment

Dissipated energy is described by:

$$\Delta E = -D\Delta x \quad (6.1)$$

Where  $D$  is dissipated energy per unit of length. Dissipated energy is assumed to be proportional with incoming energy  $E$ :

$$D = f \cdot E \quad (6.2)$$

Combining Eq. (6.1) and Eq. (6.2) gives

$$\Delta E = -f \cdot E \cdot \Delta x \quad (6.3)$$

Rewriting gives:

$$\frac{\Delta E}{\Delta x} = -f \cdot E \quad (6.4)$$

With infinitesimal small  $\Delta x$  this is rewritten as:

$$\frac{\partial E}{\partial x} = -f \cdot E \quad (6.5)$$

General solution of Eq (6.5) is given by:

$$E = E_0 \cdot e^{-f \cdot x} \quad (6.6)$$

or

$$\frac{E}{E_0} = e^{-f \cdot x} \quad (6.7)$$

Dissipation coefficient  $C_{\text{diss}}$  is defined as:

$$C_{diss} = \sqrt{\frac{E_{diss}}{E_0}} = \sqrt{\frac{E_0 - E}{E_0}} = \sqrt{1 - \frac{E}{E_0}} \quad (6.8)$$

Combining Eq. (6.7) and Eq. (6.8) gives

$$C_{diss} = \sqrt{1 - e^{-fx}} \quad (6.9)$$

Eq. (6.9) is graphical presented in Figure G.2.

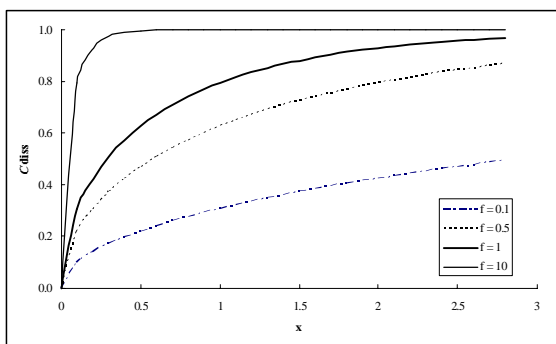


Figure G.2 Graphical presentation of dissipation coefficient based on Eq. (6.9)

## H Calculation tool

A calculation tool is developed. An impression is given in Figure H.1 and Figure H.2. User fills in mattress ( $w$ ,  $d$ ) and hydraulic conditions ( $h$ ,  $H_{m0}$ ,  $L_p$ ). All relevant parameters will be calculated. The prediction model tool also compares several dimensionless parameters with dimensionless parameters that were applied during physical model tests.

**Determination of wave transmission coefficients of brush wood mattresses**

- This sheet can be used for a first estimate of wave transmission of a floating brushwood mattress. Used formulas in this sheet are based on empirical data obtained with large scale physical modelling in Deltares Deltalume. The amount of empirical data obtained in this flume is limited. Therefore, care should be taken when using this sheet for situations which are different than tested. For detailed modelling it is strongly recommended to perform additional analysis or physical model tests.

- A description of the physical model tests and foundation of the formulas used in this sheet is given in Deltares report "Large scale physical modelling of wave damping of brushwood"

version 29 July 2011  
P. van Steeg, Deltares

**Input**

Mattress conditions			
length of mattress	$w$	100 m	WARNING: outside range of tested conditions
depth of mattress in water	$d$	0.6 m	WARNING: outside range of tested conditions
coefficient	$f$	2.4 -	
Hydraulic conditions			
water depth at mattress	$h$	6 m	WARNING: outside range of tested conditions
significant wave height	$H_{m0}$	1 m	WARNING: outside range of tested conditions
local wave length	$L_p$	33.3 m	WARNING: outside range of tested conditions

Output	Formula			
wave number	$k$	0.19 rad/m	Eq. 1	$k = \frac{2\pi}{L_p}$
energy blocking ratio	$\chi_{BL}$	0.173 -	Eq. 2	$\chi_{BL} = \frac{\sinh 2kh - \sinh 2k(h-d) + 2kd}{\sinh 2kh + 2kh}$
dim. parameter	$R$	0.52 -	Eq. 3	$R = \chi_{BL} \frac{w}{L_p}$
reflection coefficient	$C_r$	0.10 -	Eq. 4	$C_r = 0.1$
dissipation coefficient	$C_{diss}$	0.84 -	Eq. 5	$C_{diss} = \sqrt{1 - e^{-f \frac{2\pi w}{L_p}}}$
transmission coefficient	$C_t$	0.53 -	Eq. 6	$C_t = \sqrt{e^{-f \frac{2\pi w}{L_p}} - C_r^2}$
<b>transmitted wave height</b>	<b><math>H_{mo,tr}</math></b>	<b>0.53 m</b>	Eq. 7	$H_{mo,tr} = C_{tr} H_{mo,i}$

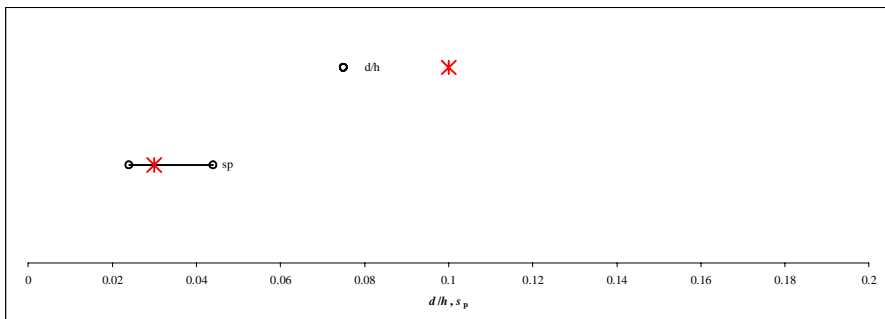
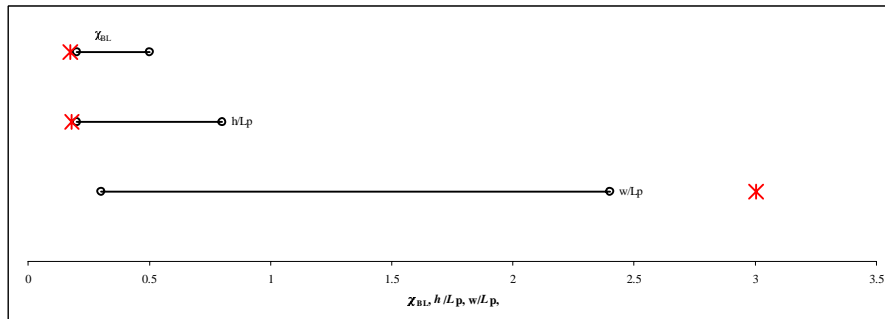
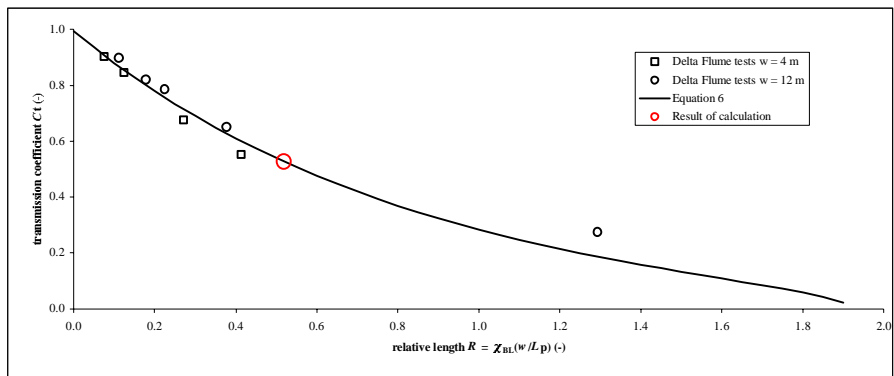
  

**Output (Dimensionless parameter)**

ratio mattress length and wave length	$w/L_p$	3.0 -	WARNING: outside range of tested conditions
ratio mattress depth and water depth	$d/h$	0.10 -	WARNING: outside range of tested conditions
ratio water depth and wave length	$h/L_p$	0.18 -	WARNING: outside range of tested conditions
wave steepness based on local water peak period	$s_p$	0.03 -	
ratio blocked wave energy	$\chi_{BL}$	0.17 -	WARNING: outside range of tested conditions

Page 1/2
[www.deltares.nl](http://www.deltares.nl)

Figure H.1 Impression of calculation tool (page 1/2)



Black line indicates test range conditions of flume test on which the prediction model is based.

Red marker indicates calculated parameter based on input prediction model

Figure H.2 Impression of calculation tool (page 2/2)



